

1 **Large but decreasing effect of ozone on the European carbon**

2 **sink**

3 Rebecca J Oliver¹, Lina M Mercado^{1,2}, Stephen Sitch², David Simpson^{3,4}, Belinda E Medlyn⁵,

4 Yan-Shih Lin⁵, Gerd A Folberth⁶

5

6 ¹ Centre for Ecology and Hydrology, Benson Lane, Wallingford, OX10 8BB, UK

7 ² College of Life and Environmental Sciences, University of Exeter, EX4 4RJ, Exeter, UK

8 ³ EMEP MSC-W Norwegian Meteorological Institute, PB 43, NO-0313, Oslo, Norway

9 ⁴ Dept. Space, Earth & Environment, Chalmers University of Technology, Gothenburg, SE-41296 Sweden

10 ⁵ Hawkesbury Institute for the Environment, Western Sydney University, Locked Bag 1797, Penrith NSW 2751

11 Australia

12 ⁶ Met Office Hadley Centre, Exeter, UK.

13 *Correspondence to:* Rebecca Oliver (rfu@ceh.ac.uk)

14

15

16

17

18

19

20

21

22

23

24

25

26 **Abstract**

27

28 The capacity of the terrestrial biosphere to sequester carbon and mitigate climate change is governed by the ability
29 of vegetation to remove emissions of CO₂ through photosynthesis. Tropospheric O₃, a globally abundant and
30 potent greenhouse gas, is, however, known to damage plants, causing reductions in primary productivity, yet the
31 impact of this gas on European vegetation and the land carbon sink is largely unknown. Despite emission control
32 policies across Europe, background concentrations of tropospheric O₃ have risen significantly over the last
33 decades due to hemispheric-scale increases in O₃ and its precursors. Therefore, plants are exposed to increasing
34 background concentrations, at levels currently causing chronic damage. We use the JULES land-surface model
35 recalibrated for O₃ impacts on European vegetation, with an improved stomatal conductance parameterization, to
36 quantify the impact of tropospheric O₃, and its interaction with CO₂, on gross primary productivity (GPP) and
37 land carbon storage across Europe. A factorial set of model experiments showed that tropospheric O₃ can
38 ~~significantly~~ suppress terrestrial carbon uptake across Europe over the period 1901 to 2050. ~~By 2050, simulated~~
39 ~~GPP was reduced by 4 to 9% due to plant ozone damage and land carbon storage by 3 to 7%.~~ ~~However, the~~
40 ~~combined physiological effects of elevated future CO₂ (acting to reduce stomatal opening) and reductions in O₃~~
41 ~~concentrations resulted in reduced O₃ damage in the future, contrary to predictions from earlier studies. This~~
42 ~~alleviation of O₃ damage by CO₂ induced stomatal closure was around 1 to 2% for low and high sensitivity~~
43 ~~respectively (on both land carbon and GPP). Reduced land carbon storage resulted from diminished soil carbon~~
44 ~~stocks consistent with the reduction in GPP. Regional variations are identified with larger impacts shown for~~
45 ~~temperate Europe (GPP reduced by 10 to 20%) compared to boreal regions (GPP reduced by 2 to 8%). These~~
46 ~~results highlight that O₃ damage needs to be considered when predicting GPP and land carbon, and that the effects~~
47 ~~of O₃ on plant physiology need to be considered in regional -add to the uncertainty of future trends in the land~~
48 ~~carbon cycle assessments. sink, and, as such, this should be incorporated into carbon cycle assessments.~~

49

50

51

52

53

54

55

56

57

58

Commented [ORJ1]: RC1 1):

RC1 2):

59 **1 Introduction**

60
61 The terrestrial biosphere absorbs around 30% of anthropogenic CO₂ emissions and acts to mitigate climate change
62 (Le Quéré et al., 2015). Early estimates of the European carbon balance suggest a terrestrial carbon sink of between
63 135 to 205 TgC yr⁻¹ (Janssens et al., 2003). Schulze et al. (2009) determined a larger carbon sink of 274 TgC yr⁻¹,
64 and more recent estimates suggest a European terrestrial sink of between 146 to 184 TgC yr⁻¹ (Luyssaert et al.,
65 2012). The carbon sink capacity of land ecosystems is dominated by the ability of vegetation to sequester carbon
66 through photosynthesis and release it back to the atmosphere through respiration. Therefore, any change in the
67 balance of these fluxes will alter ecosystem source-sink behaviour.

68
69 In recent decades much attention has focussed on the effects of rising atmospheric CO₂ on vegetation productivity
70 (Ceulemans and Mousseau, 1994;Norby et al., 2005;Norby et al., 1999;Saxe et al., 1998). The Norby et al. (2005)
71 synthesis of Free Air CO₂ Enrichment (FACE) experiments suggests a median stimulation (23 ± 2%) of forest
72 NPP in response to a doubling of CO₂. Similar average increases (20%) were observed for C₃ crops, although this
73 translated into smaller gains in biomass (17%) and crop yields (13%) (Long et al., 2006). ~~The long-term effects~~
74 ~~of CO₂ fertilization on plant growth and carbon storage are nevertheless uncertain (Baig et al., 2015;Ciais et al.,~~
75 ~~2013).~~ Little attention, however, has been given to tropospheric ozone (O₃), a globally abundant ~~and increasing~~
76 air pollutant recognised as one of the most damaging pollutants for forests (Karlsson et al., 2007;Royal-Society,
77 2008;Simpson et al., 2014b). Tropospheric O₃ is a secondary air pollutant formed by photochemical reactions
78 involving carbon monoxide (CO), volatile organic compounds (VOCs), methane (CH₄) and nitrogen oxides (NO_x)
79 from both man-made and natural sources, as well as downward transport from the stratosphere ~~and lightning~~
80 ~~which is a source of NO_x~~. The phytotoxic effects of O₃ exposure are shown to decrease vegetation productivity
81 and biomass, with consequences for terrestrial carbon sequestration (Felzer et al., 2004;Loya et al., 2003;Mills et
82 al., 2011b;Sitch et al., 2007). Few studies, however, consider the simultaneous effects of exposure to both gases,
83 and few Earth-system models (ESMs) currently explicitly consider the role of tropospheric O₃ in terrestrial carbon
84 dynamics (IPCC, 2013), both of which are key to understanding the carbon sequestration potential of the land-
85 surface, and future carbon dynamics regionally and globally.

86
87 Due to increased anthropogenic precursor emissions over the industrial period, background concentrations of
88 ground-level O₃ have risen (Vingarzan, 2004) (Parrish et al., 2012). ~~O₃ levels at the start of the 20th century are~~
89 ~~estimated to be around 10 ppb for the site Montsouris Observatory near Paris, data for Arkona on the Baltic coast~~
90 ~~increased from ca. 15 ppb in the 1950s to 20-27 ppb by the early 1980s, and the Irish coast site Mace Head shows~~
91 ~~around 40 ppb by the year 2000 (Logan et al., 2012;Parrish et al., 2012). Present day annual average background~~
92 ~~O₃ concentrations reported in the review of (Vingarzan, 2004) show O₃ concentrations range between~~
93 ~~approximately 20 and 45ppb, with the greatest increase occurring since the 1950s. Trends vary from site to site~~
94 ~~though, even on a decadal basis (Logan et al., 2012;Simpson et al., 2014b), depending, for example, on~~
95 ~~local/regional trends in precursor (especially NO_x) emissions, elevation, and exposure to long-range transport.~~
96 ~~Nevertheless, there is some indication that background O₃ levels over the mid-latitudes of the Northern~~
97 ~~Hemisphere have continued to rise at a rate of approximately 0.5–2% per year, although not uniform (Vingarzan,~~
98 ~~2004).~~ As a result of controls on precursor emissions in Europe and North America, peak O₃ concentrations in

Commented [ORJ2]: RC2 minor comment 2.

Commented [ORJ3]: RC2 minor comment 3.

Commented [ORJ4]: RC1 5)

99 these regions have decreased or stabilised over recent decades (Cooper et al., 2014; Logan et al., 2012; Parrish et
100 al., 2012; Simpson et al., 2014b). Nevertheless, climate change may increase the frequency of weather events
101 conducive to peak O₃ incidents in the future (e.g. summer droughts and heat-waves; e.g., (Sicard et al., 2013), and
102 may increase biogenic emissions of the O₃-precursors isoprene and NO_x, although such impacts are subject to
103 great uncertainty (Simpson et al., 2014b; Young et al., 2013; Young et al., 2009). ~~Furthermore, intercontinental~~
104 ~~transport of air pollution- from regions such as Asia that currently have poor emission controls are thought to~~
105 ~~contribute substantially to rising means~~ background O₃ concentrations ~~have risen significantly~~ over the last
106 decades (Cooper et al., 2010; Verstraeten et al., 2015). Northern Hemisphere background concentrations of O₃ are
107 now close to established levels for impacts on human health and the terrestrial environment (Royal-Society, 2008).
108 Therefore, although peak O₃ concentrations are in decline across Europe, plants are exposed to increasing
109 background levels, at levels currently causing chronic damage (Mills et al., 2011b). Intercontinental transport
110 means future O₃ concentrations in Europe are dependent on how O₃ precursor emissions evolve globally ~~;~~
111 ~~including regions such as Asia that currently have poor emission controls~~ (Cooper et al., 2010; Verstraeten et al.,
112 2015).

Commented [ORJ5]: RC2 minor comment 4.

Field Code Changed

113
114 Elevated O₃ concentrations impact agricultural yields and nutritional quality of major crops (Ainsworth et al.,
115 2012; Avnery et al., 2011), with consequences for global food security (Tai et al., 2014). As well as being a
116 significant air pollutant, O₃ is a potent greenhouse gas (Royal-Society, 2008). High levels of O₃ are damaging to
117 ecosystem health and reduce the global land carbon sink (Armeth et al., 2010; Sitch et al., 2007). Reduced uptake
118 of carbon by plant photosynthesis due to O₃ damage allows more CO₂ to remain in the atmosphere. This effect of
119 O₃ on plant physiology represents an additional climate warming to the direct radiative forcing of O₃ (Collins et
120 al., 2010; Sitch et al., 2007), the magnitude of which, however, remains highly uncertain (IPCC, 2013).

Commented [ORJ6]: RC2 minor comment 5.

Commented [ORJ7]: RC2 minor comment 6.

121
122 Dry deposition of O₃ to terrestrial surfaces, primarily uptake by stomata on plant foliage and deposition on external
123 surfaces of vegetation, is a ~~large significant~~ sink for ground level O₃ (Fowler et al., 2009; Fowler et al., 2001). On
124 entry to sub-stomatal spaces, O₃ reacts with other molecules to form reactive oxygen species (ROS). Plants can
125 tolerate a certain level of O₃ depending on their capacity to scavenge and detoxify the ROS (Ainsworth et al.,
126 2012). Above this critical level, long-term chronic O₃ exposure reduces plant photosynthesis and biomass
127 accumulation (Ainsworth, 2008; Ainsworth et al., 2012; Matyssek et al., 2010a; Wittig et al., 2007; Wittig et al.,
128 2009), either directly through effects on photosynthetic machinery such as reduced Rubisco content (Ainsworth
129 et al., 2012; Wittig et al., 2009) and/or indirectly by reduced stomatal conductance (g_s) (Kitao et al., 2009; Wittig
130 et al., 2007), alters carbon allocation to different pools (Grantz et al., 2006; Wittig et al., 2009), accelerates leaf
131 senescence (Ainsworth, 2008; Nunn et al., 2005; Wittig et al., 2009) and changes plant susceptibility to biotic stress
132 factors (Karnosky et al., 2002; Percy et al., 2002).

Commented [ORJ8]: RC2 minor comment 7.

133
134 The response of plants to O₃ is very wide ranging as reported in the literature from different field studies. We
135 compare results from the present study to values found in literature. The Wittig et al. (2007) meta-analysis of
136 temperate and boreal tree species showed future concentrations of O₃ predicted for 2050 significantly reduced leaf
137 level light saturated net photosynthetic uptake (-19%, range: -3% to -28%) and g_s (-10%, range: +5% to -23%) in
138 both broadleaf and needle leaf tree species. In the Feng et al. (2008) meta-analysis of wheat, projected O₃

139 concentrations for the future reduced aboveground biomass (-18%), CI (-13% to -24%), photosynthetic rate (-
140 20%) and g_s (-22%). One of few long-term field based O₃ exposure studies (AspenFACE) showed that after 11
141 years of exposing mature trees to elevated O₃ concentrations, O₃ decreased ecosystem carbon content (-9%), and
142 decreased NPP (-10%), although the O₃ effect decreased through time (Talhelm et al., 2014). Zak et al. (2011)
143 showed this was partly due to a shift in community structure as O₃-tolerant species, competitively inferior in low
144 O₃ environments, out competed O₃-sensitive species. Zak et al. (2011) GPP was reduced (-12% to -19%) at two
145 Mediterranean ecosystems exposed to elevated O₃ (dominated by either *Pinus* species or *Citrus* species)-studied
146 by Fares et al. (2013). Biomass of mature beech trees was reduced (-44%) after 8 years of exposure to elevated
147 O₃ (Matyssek et al., 2010a). After 5 years of O₃ exposure in a semi-natural grassland, annual biomass production
148 was reduced (-23%), and in a Mediterranean annual pasture O₃ exposure significantly reduced total aboveground
149 biomass (up to -25%) (Calvete-Sogo et al., 2014). However, these were empirical studies at individual sites, and
150 these focus on O₃ effects on plant physiology and productivity, but do not quantify the impact on the land carbon
151 sink. Modelling studies are needed to scale site observations to the regional and global scales. Models generally
152 suggest that plant productivity and carbon sequestration will decrease with O₃ pollution, though the magnitudes
153 vary. For example, based on a limited dataset to parameterise plant O₃ damage for a global set of plant functional
154 types, Sitch et al. (2007) predicted a decline in global GPP of 14 to 23% by 2100. A second study by Lombardozzi
155 et al. (2015) similarly predicted a 10.8% decrease of global GPP. Here we take a regional approach and take
156 advantage of new measurements specifically for European vegetation and conduct a dedicated analysis for the
157 European region. Results from the present study suggest projected O₃ concentrations for 2050 will reduce mean
158 GPP for Europe (-4% to -9%), NPP (-6% to -11%), total carbon content (-3% to -7%) and g_s (-4% to -9%). Using
159 GPP as a proxy for A_{gross} (these variables are not identical but they are related), our mean GPP and g_s estimates fall
160 within the range given by the meta-analysis of Wittig et al. (2007). The remaining studies are not meta-analyses,
161 so are site- and species-specific, our estimates appear to compare more conservatively with these, however these
162 are a mean value for Europe and spatially our estimates show greater variability.

Commented [ORJ9]: RC1 3/4/6)

165 Understanding the response of plants to elevated tropospheric O₃ is challenged by the large variation in O₃
166 sensitivity both within and between species (Karnosky et al., 2007; Kubiske et al., 2007; Wittig et al., 2009).
167 Additionally, other environmental stresses that affect stomatal behaviour will affect the rate of O₃ uptake and
168 therefore the response to O₃ exposure, such as high temperature, drought and changing concentrations of
169 atmospheric CO₂ (Mills et al., 2016; Fagnano et al., 2009; Kitao et al., 2009; Löw et al., 2006), such that the
170 response of vegetation to O₃ is a balance between opposing drivers of stomatal behaviour. Increasing
171 concentrations of atmospheric CO₂, for example, are suggested to provide some protection against O₃ damage by
172 causing stomata to close (Harmens et al., 2007; Wittig et al., 2007), however the long-term effects of CO₂
173 fertilisation. The long-term effects of CO₂ fertilization on plant growth and carbon storage remain are nevertheless
174 uncertain (Baig et al., 2015; Ciais et al., 2013). Further, in some studies, stomata have been shown to respond
175 sluggishly, losing their responsiveness to environmental stimuli with exposure to O₃ which can lead to higher O₃
176 uptake, increased water-loss and therefore greater vulnerability to environmental stresses such as drought (Mills
177 et al., 2016; Mills et al., 2009; Paoletti and Grulke, 2010; Wilkinson and Davies, 2009).Mention uncertainties

Field Code Changed

178 around CO₂ fertilisation here, nutrient cycling and stomatal sluggishness here. Maybe introduce Medlyn model
179 here

Commented [ORJ10]: RC2 6)

180
181 Given the critical role g_s plays in the uptake of both CO₂ and O₃, we use an alternative improved representation
182 and parameterisation of g_s in JULES by implementing the Medlyn *et al.* (2011) g_s formulation. This model is
183 based on the optimal theory of stomatal behaviour, it does not currently include a representation of sluggish
184 stomatal control, but it Medlyn *et al.* (2011) has the following advantages over the current JULES g_s formulation
185 of Jacobs (1994): i) a single parameter (g_1) which represents the marginal cost of water-use, compared to two
186 parameters in Jacobs (1994) representing the the critical humidity deficit at the leaf surface (d_{crit}) and the ci/ca
187 ratio at the leaf critical humidity deficit (f_l) (Clark *et al.*, 2011); ii) easier to parameterise with leaf or canopy
188 level observations of photosynthesis, g_s and humidity – all variables that are commonly measured, and (iii) values
189 of g_1 are available for many different plant functional types (PFTs) derived from a global data set of measured
190 leaf-level measurements stomatal conductance, photosynthesis and vapour pressure deficit (VPD) (Lin *et al.*
191 2015).

Commented [ORJ11]: RC2 3)

192
193 Here weThe main objective of this work is to assess the impact of historical and projected (1901 to 2050)
194 changes in tropospheric O₃ and atmospheric CO₂ concentration from 1901 to 2050 on the predicted GPP and the
195 European land-carbon sink for Europe. These are the two greenhouse gases that directly affect plant
196 photosynthesis and g_s . We use a factorial suite of model experiments, using the Joint UK land environment
197 simulator (JULES) (Best *et al.*, 2011; Clark *et al.*, 2011), the land-surface model of the UK Earth System Model
198 (UKESM) (Collins *et al.*, 2011) to simulate plant O₃ uptake and damage, and to look at the interaction between
199 O₃ and CO₂. In this work, plant O₃ damage in JULES is developed further by introducing a term for dry
200 deposition of O₃ to external plant surfaces, an important sink for tropospheric O₃ that was previously absent
201 from the model. Further, the model is re-calibrated using the latest observations of vegetation sensitivity to O₃,
202 with the addition of a separate parameterisation for temperate/boreal regions versus the Mediterranean. The
203 plant O₃ sensitivity of each PFT in JULES was re-calibrated for both a (high and low plant O₃ sensitivity to
204 account for the large variation in O₃ sensitivity within and between species.) using the latest observations for
205 European vegetation in order to capture a range of plant sensitivities to O₃—(This includes separate sensitivities
206 for Mediterranean regions, and for agricultural crops (wheat) versus natural grassland. We make a separate
207 distinction for the Mediterranean region where possible because the work of Büker *et al.* (2015) showed that
208 different O₃ dose-response relationships are needed to describe the O₃ sensitivity of dominant Mediterranean
209 trees. We modify the representation of stomatal O₃ flux in JULES from Sitch *et al.*, (2007) by including a term
210 for non-stomatal deposition of O₃ to leaf surfaces which is recognised as an important sink for ground-level
211 O₃. In addition, we introduce an alternative g_s scheme into JULES as described above. JULES is forced with
212 spatially varying hourly O₃ concentrations from a high resolution atmospheric chemistry model for Europe,
213 therefore our simulations account for diurnal variations in O₃ concentration and O₃ responses allowing for more
214 accurate estimations of O₃ uptake by vegetation. We do not attempt to make a full assessment of the carbon
215 cycle of Europe, instead we target O₃ damage, and its interaction with CO₂, which is currently a missing
216 component in earlier carbon cycle assessments (Le Quéré *et al.*, 2017; Sitch *et al.*, 2015). To this end, we
217 prescribe changing O₃ and CO₂ concentrations from 1901 to 2050, but use a fixed pre-industrial climate. We

Commented [ORJ12]: RC2 minor comment 8.

218 acknowledge the use of a 'fixed' pre-industrial climate omits the additional uncertainty of the interaction
219 between climate change and g_s , which will affect the rate of O_3 uptake and therefore O_3 concentrations. To
220 understand the impact of these complex feedback mechanisms is an important area for future work, but in the
221 current study our aim is to isolate the physiological response of plants to both O_3 and CO_2 , and determine the
222 sensitivity of predicted GPP and the land carbon sink to this process, as the impact of O_3 on European
223 vegetation and the land carbon sink currently remains largely unknown.]

224 Given the critical role g_s plays in the uptake of both CO_2 and O_3 , we use an improved representation and
225 parameterisation of g_s in JULES by implementing the Medlyn *et al.* (2011) g_s formulation. Based on the optimal
226 theory of stomatal behaviour, Medlyn *et al.*, (2011) has the following advantages over the current JULES g_s
227 formulation: i) a single parameter (g_{s0}) which represents the marginal cost of water use; ii) easy to parameterise
228 with leaf or canopy level observations, and (iii) values of g_s are available for different plant functional types
229 (PFTs) derived from a global data set of measured leaf stomatal conductance, photosynthesis and vapour pressure
230 deficit (VPD) (Lin *et al.*, 2015).

231
232 We use a factorial suite of model experiments to investigate the temporal and spatial evolution of O_3 impacts on
233 European vegetation from 1901 to 2050. We do not attempt to make a full assessment of the carbon cycle of
234 Europe, instead we target O_3 damage which is currently a missing component in earlier carbon cycle assessments.
235 Accounting for the well-known differences in plant sensitivity to O_3 is complex, therefore, here we provide a
236 sensitivity assessment by using two sets of simulations—a high and lower plant O_3 sensitivity parameterisation,
237 with O_3 sensitivities that vary by PFT and region. We investigate the interaction between CO_2 and O_3 , the two
238 greenhouse gases that directly affect plant photosynthesis, and indirectly g_s . Our aim is to quantify the impact of
239 these two gases on GPP and land carbon storage across Europe. We go beyond the present day carbon budget and
240 investigate the impact of state of art future scenarios up to year 2050.

241 242 2 Methods

243 244 2.1 Representation of O_3 effects in JULES

245
246 JULES calculates the land-atmosphere exchanges of heat, energy, mass, momentum and carbon on a sub-daily
247 time step, and includes a dynamic vegetation model (Best *et al.*, 2011; Clark *et al.*, 2011; Cox, 2001). [This work
248 uses JULES version 3.3 (<http://www.jchmr.org>) at $0.5^\circ \times 0.5^\circ$ spatial resolution and hourly model time step, the
249 spatial domain is shown in Fig. S5.] JULES which has uses a multi-layer canopy radiation interception and
250 photosynthesis scheme (10 layers in this instance) that accounts for direct and diffuse radiation, sun fleck
251 penetration through the canopy, inhibition of leaf respiration in the light and change in photosynthetic capacity
252 with depth into the canopy (Clark *et al.*, 2011; Mercado *et al.*, 2009). Soil water content also affects the rate of
253 photosynthesis and g_s . It is modelled using a dimensionless soil water stress factor, β , which is related to the mean
254 soil water concentration in the root zone, and the soil water contents at the critical and wilting point (Best *et al.*,
255 2011).

256

Commented [ORJ13]: RC1 2)

Commented [ORJ14]: RC2 1)

Commented [ORJ15]: RC2 minor comment 9.

257 To simulate the effects of O₃ deposition on vegetation productivity and water use, JULES uses the flux-gradient
 258 approach of Sitch *et al.*, (2007), modified to include non-stomatal deposition following Tuovinen *et al.* (2009).
 259 JULES uses a coupled model of g_s and photosynthesis; because of the relationship between these two fluxes, the
 260 direct effect of O₃ damage on photosynthetic rate also leads to a reduction in g_s . Changes in atmospheric CO₂
 261 concentration also affect photosynthetic rate and g_s , consequently the interaction between changing concentrations
 262 of both gases is allowed for. Specifically, the potential net photosynthetic rate (A_p , mol CO₂ m⁻² s⁻¹) is modified
 263 by an 'O₃ uptake' factor (F , the fractional reduction in photosynthesis), so that the actual net photosynthesis (A_{net} ,
 264 mol CO₂ m⁻² s⁻¹) is given by equation 1 (Clark *et al.*, 2011, Sitch *et al.*, 2007).

$$265 \quad A_{net} = A_p F \quad (1)$$

266 The O₃ uptake factor (F) is defined as:

$$269 \quad F = 1 - a * \max[F_{O_3} - F_{O_3crit}, 0.0] \quad (2)$$

270 F_{O_3} is the instantaneous leaf uptake of O₃ (nmol m⁻² s⁻¹), F_{O_3crit} is a PFT-specific threshold for O₃ damage (nmol
 271 m⁻² PLA s⁻¹, projected leaf area), and 'a' is a PFT-specific parameter representing the fractional reduction of
 272 photosynthesis with O₃ uptake by leaves. Following Tuovinen *et al.* (2009), the flux of O₃ through stomata, F_{O_3} ,
 273 is represented as follows:

$$274 \quad F_{O_3} = O_3 \left(\frac{g_b \left(\frac{g_l}{K_{O_3}} \right)}{g_b + \left(\frac{g_l}{K_{O_3}} \right) + g_{ext}} \right) \quad (3a)$$

275 O_3 is the molar concentration of O₃ at reference (canopy) level (nmol m⁻³), g_b is the leaf-scale boundary layer
 276 conductance (m s⁻¹, eq 3b), g_l is the leaf conductance for water (m s⁻¹), K_{O_3} accounts for the different diffusivity of
 277 ozone to water vapour is the ratio of leaf resistance for O₃ to leaf resistance for water vapour and takes a value of
 278 1.51 after Massman (1998), and g_{ext} is the leaf-scale non-stomatal deposition to external plant surfaces (m s⁻¹)
 279 which takes a constant value of 0.0004 m s⁻¹ after Tuovinen *et al.* (2009). The leaf-level boundary layer
 280 conductance (g_b) is calculated as in Tuovinen *et al.* (2009)

$$281 \quad g_b = \alpha L d^{-1/2} U^{-1/2} \quad (3b)$$

282 α is a constant (0.0051 m s^{1/2}), Ld is the cross-wind leaf dimension (m) and U is wind speed at canopy height (m
 283 s⁻¹). The rate of O₃ uptake is dependent on g_s , which is dependent on photosynthetic rate. Given g_s is a linear
 284 function of photosynthetic rate in JULES (Clark *et al.*, 2011), from eq 1 it follows that:

$$285 \quad g_s = g_l F \quad (4)$$

286 The O₃ flux to stomata, F_{O_3} , is calculated at leaf level and then scaled to each canopy layer differentiating sunlit
 287 and shaded leaf photosynthesis, and finally summed up to the canopy level. Because the photosynthetic capacity,

Commented [ORJ16]: RC2 minor comment 10.

296 photosynthesis and therefore g_s decline with depth into the canopy, this in turn affects O_3 uptake, with the top leaf
297 level contributing most to the total O_3 flux and the lowest level contributing least.

298

299 **2.2 Calibration of O_3 uptake model for European vegetation**

300

301 Here we use the latest literature on O_3 dose-response relationships derived from observed field data across Europe
302 (CLRTAP, 2017) to determine the key PFT-specific O_3 sensitivity parameters in JULES (a and F_{O_3crit}). Each
303 JULES PFT (broadleaf, needle leaf, C_3 and C_4 herbaceous, and shrub) was calibrated for a high and low plant O_3
304 sensitivity to account for uncertainty in variation of species sensitivity to O_3 , using the approach of Sitch *et al.*,
305 (2007). For the C_3 herbaceous PFT – the dominant land cover type across Europe in this study (Fig. S1) - the O_3
306 sensitivity was calibrated against observations for wheat to give a representation of agricultural regions (high plant
307 O_3 sensitivity), versus natural grassland (low plant O_3 sensitivity), with a separate function for Mediterranean
308 grasslands (low plant O_3 sensitivity) (Table S1 and Figure S2). Broadleaf tree and shrub PFTs were calibrated
309 against the birch/beech observed O_3 dose-response functions for the high plant O_3 sensitivity, with a separate
310 function for Mediterranean broadleaf trees (deciduous oaks), needle leaf trees were calibrated against the function
311 for Norway spruce, all data for dose-response functions were from CLRTAP (2017). The low plant O_3 sensitivity
312 functions for trees/shrubs were calibrated as being 20% less sensitive based on the difference in sensitivity
313 between high and low sensitive tree species in the Karlsson *et al.* (2007) study. Due to limitations in data
314 availability, the parameterisation for C_4 herbaceous uses the observed dose-responses for C_3 herbaceous, however
315 the fractional cover of C_4 herbs across Europe is low (Fig. S1), so this assumption affects a very small percentage
316 of land cover.

317

318 To calibrate each JULES PFT for sensitivity to O_3 , JULES was run, varying the value of parameter a , until model
319 output of change in NPP with cumulative O_3 exposure matched the observed O_3 dose-response functions in
320 CLRTAP (2017).

321 To calibrate the JULES O_3 sensitivity (parameter ' a ' in eq 2), JULES was run to be as directly comparable as
322 possible to the dose-based O_3 risk indicator used in CLRTAP (2017), using the O_3 flux per projected leaf area to
323 top canopy sunlit leaves. Hourly averaged F_{O_3} in excess of F_{O_3crit} were accumulated over a species specific
324 accumulation period. Values of F_{O_3crit} came from the observations, the parameter ' a ' was modified until the
325 modelled change in response variable with cumulative uptake of O_3 above the specified threshold matched the
326 observations (see further method details in SI section S2).

327

328 **2.3 Representation of stomatal conductance**

329

330 In JULES, g_s ($m s^{-1}$) is represented following the closure proposed by (Jacobs, 1994):

331

$$332 g_s = 1.6RT_l \frac{A_{net}\beta}{c_a - c_t} \quad (5)$$

333

334 In this parameterisation, c_t is unknown and where in the default JULES model is calculated as in equation 6,
335 hereafter called JAC:

Commented [ORJ17]: RC2 3)

336

$$337 \quad c_i = (c_a - c_s) f_0 \left(1 - \frac{dq}{dq_{crit}} \right) + c_s \quad (6)$$

338

339 β is a soil moisture stress factor, the factor 1.6 accounts for g_s being the conductance for water vapour rather than
340 CO_2 , R is the universal gas constant ($\text{J K}^{-1} \text{mol}^{-1}$), T_l is the leaf surface temperature (K), c_a and c_i (both Pa) are the
341 leaf surface and internal CO_2 partial pressures, respectively, c^* (Pa) is the CO_2 photorespiration compensation
342 point, dq is the humidity deficit at the leaf surface (kg kg^{-1}), dq_{crit} (kg kg^{-1}) and f_0 are PFT specific parameters
343 representing the critical humidity deficit at the leaf surface, and the leaf internal to atmospheric CO_2 ratio (c_i/c_a)
344 at the leaf specific humidity deficit (Best *et al.* 2011), values are shown in Table S1.

345

346 In this work, we replace equation 6 with the closure described in Medlyn *et al.* (2011), closure using the key PFT
347 specific model parameter g_l ($\text{kPa}^{0.5}$), and dq is expressed in kPa, shown in eq 7, hereafter called MED:

348

$$349 \quad c_i = c_a \left(\frac{g_l}{g_l + \sqrt{dq}} \right) \quad (7)$$

350

351 PFT specific values of the g_l parameter were derived for European vegetation from the data base of Lin *et al.*
352 (2015) and are shown in Table S1. The g_l parameter represents the sensitivity of the g_s to the assimilation rate,
353 i.e. plant water use efficiency, and it was derived as in Lin *et al.* (2015) by fitting the Medlyn *et al.*, (2011)
354 model to observations of g_s , photosynthesis, and VPD, with no g_0 term (Lin *et al.*, 2015). The study of Hoshika *et al.*
355 (2013) show a significant difference in the g_l parameter (higher in elevated O_3 compared to ambient) in
356 Siebold's beech in June of their experiment. However, this is only at the start of the growing season, further
357 measurements show no difference in this parameter between O_3 treatments. found an effect of O_3 on g_l for beech
358 trees (*Fagus sylvatica*) only at the start of the growing season (June), but not during the following months (August
359 and October). Quantifying an O_3 effect directly on g_l would require a detailed meta-analysis of empirical data on
360 photosynthesis and g_s for different PFTs, which is currently lacking in the literature. As explained above, here we
361 take an empirical approach to modelling plant O_3 damage, essentially by applying a reduction factor to the
362 simulated plant photosynthesis based on observations of whole plant losses of biomass with O_3 exposure, for
363 which there is a lot more available data (e.g. CLRTAP, 2017). The impact of the g_s model formulation is shown
364 for two contrasting grid points (wet/dry) in central Europe (see SI section S3 for further details). We also carry
365 out site level evaluation of the two g_s models compared to FLUXNET observations (see SI section S4).

366

367 2.4 Model simulations for Europe

368

369 2.4.1 Forcing datasets

370

371 We used the WATCH meteorological forcing data set (Weedon *et al.*, 2010; Weedon *et al.*, 2011) at $0.5^\circ \times 0.5^\circ$
372 spatial and three hour temporal resolution for our JULES simulations. JULES interpolates this down to an hourly
373 model time step. For this study, the climate was kept constant by recycling over the period 1901 to 1920, to allow
374 us to fully understand the impact O_3 , CO_2 and their interaction.

Commented [ORJ18]: RC2 minor comment 12.

Commented [ORJ19]: RC2 minor comment 12.

Commented [ORJ20]: RC2 minor comment 13.

Commented [ORJ21]: RC2 minor comment 19.

375
376 ~~JULES was run with prescribed annual mean atmospheric CO₂ concentrations.~~ Pre-industrial global CO₂
377 concentrations (1900 to 1960) were taken from Etheridge et al. (1996), 1960 to 2002 were from Mauna Loa
378 (Keeling and Whorf, 2004), as calculated by the Global Carbon Project (Le Quéré et al., 2016), and 2003-2050
379 were based on the IPCC SRES A1B scenario and were linearly interpolated to gap fill missing years (Fig. 1).

380
381 JULES was run including dynamic vegetation with a land cover mask giving the fraction of agriculture in each
382 ~~0.5° x 0.5° grid cell based on the Hurtt et al. (2011) land cover database for the year 2000. [Within the agricultural~~
383 ~~mask means that, only C₃/C₄ herbaceous PFTs are allowed to grow, with no competition from and all other PFTs~~
384 ~~, no form of land management is simulated are assumed absent.~~ By including dynamic vegetation, grid cell PFT
385 coverage and Leaf Area Index (LAI) is a result of resource availability and simulated competition. Following a
386 full spin-up period (to ensure equilibrium vegetation, carbon and water states), the fractional cover of each PFT
387 changed little over the simulation period (1901 - 2050), the land cover for 2050 is shown in Fig. S1. ~~The model~~
388 ~~experiments in this study are run for both a high and low plant O₃ sensitivity: for the high plant O₃ sensitivity, all~~
389 ~~herbaceous PFT fractional cover uses the O₃ sensitivity for wheat, and for the low plant O₃ sensitivity, all~~
390 ~~herbaceous PFT fractional cover uses the O₃ sensitivity for natural grasslands.~~

Commented [ORJ22]: RC2 minor comment 16.

391
392 ~~Tropospheric O₃ concentration was produced by the EMEP MSC-W model at 0.5° x 0.5° (Simpson et al., 2012),~~
393 ~~driven with meteorology from the regional climate model RCA3 (Kjellström et al., 2011; Samuelsson et al., 2011),~~
394 ~~which provides a downscaling of the ECHAM A1B-r3 (simulation 11 of Kjellström et al., 2011). This setup~~
395 ~~(EMEP+RCA3) is also used by Langner et al. (2012a), Simpson et al. (2014a), Tuovinen et al. (2013), Franz et~~
396 ~~al. (2017) and Engardt et al. (2017), where further details and model evaluation can be found. Unfortunately, the~~
397 ~~3-dimensional RCA3 data needed by the EMEP model was not available prior to 1960, but as in Engardt et al.~~
398 ~~(2017) the meteorology of 1900-1959 had to be approximated by assigning random years from 1960 to 1969. This~~
399 ~~procedure introduces some uncertainty of course, but Langner et al. (2012b) show that it is emissions change,~~
400 ~~rather than meteorological change, that drives modelled ozone concentrations. The emissions scenarios for 1900-~~
401 ~~2050 merge data from the International Institute of Applied System Analysis (IIASA) for 2005-2050 (the so-~~
402 ~~called ECLIPSE 4a scenario, Klimont et al. (2016)), recently revised EMEP data for 1990, and a scaling back~~
403 ~~from 1990 to 1900 using data from Lamarque et al. (2013). The EMEP model accounts for changes in BVOC~~
404 ~~emissions as a result of predicted ambient temperature changes, however as with all uncoupled modelling studies,~~
405 ~~there is no interaction between changes in leaf-level g_s, BVOCs and O₃ formation.~~

Commented [ORJ23]: RC2 2)

406
407 This study used daily mean values of tropospheric O₃ concentration from EMEP MSC-W disaggregated down to
408 the hourly JULES model time-step. ~~The daily mean O₃ forcing was disaggregated to follow a mean diurnal profile~~
409 ~~of O₃, this was generated from hourly O₃ output from EMEP MSC-W for the two land cover categories across the~~
410 ~~same domain as in this study.~~ Hourly O₃ values allow for variation in the diurnal response to O₃ exposure resulting
411 in more accurate estimation of O₃ uptake. O₃ concentrations from EMEP were calculated at canopy height for two
412 land-cover categories: forest and grassland (Fig. S3 and Fig. S4), which are taken as surrogates for high and low
413 vegetation, respectively. These canopy-height specific concentrations allow for the large gradients in O₃
414 concentration that can occur in the lowest 10s of metres, giving lower O₃ for grasslands than seen at e.g. 20 m in

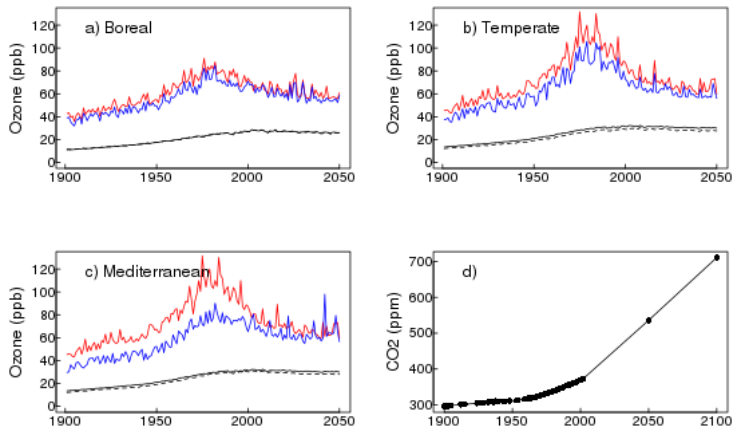
Commented [ORJ24]: RC2 minor comment 14.

415 a forest canopy (Simpson et al., 2012;Tuovinen et al., 2009). Figure 1 shows the regional mean annual O₃
416 concentration (regions are depicted in Fig. S5) along with the annual maximum. Together these clearly show the
417 trend of increasing O₃ concentration on pre-industrial levels in all regions, although notably lower increases in the
418 Boreal region. Around the 1990's O₃ concentrations stabilise and then start to decrease into the future.

419
420 Figure 1 shows large increases in tropospheric O₃ from pre-industrial to present day (2001), this is in line with
421 modelling studies (Young et al., 2013) and site observations (Derwent et al., 2008;Logan et al., 2012;Parrish et
422 al., 2012), and is predominantly a result of increasing anthropogenic emissions (Young et al., 2013). Figure's S3
423 and S4 show this large increase in ground-level O₃ concentrations from 1901 to 2001 occurs in all seasons. Present
424 day O₃ concentration show a strong seasonal cycle, with a spring/summer peak in concentrations in the mid-
425 latitudes of the Northern Hemisphere (Derwent et al., 2008;Parrish et al., 2012;Vingarzan, 2004). This is largely
426 related to the seasonal cycle of photochemical O₃ production which is highest during periods of high radiation and
427 temperature (Young et al., 2013), although increased stratospheric input is also thought to contribute (Vingarzan
428 2004). Anthropogenic emissions, especially NO_x, contribute to the seasonal cycle of O₃ through traffic, energy
429 production and residential heating and cooling demands (Royal-Society, 2008). Biogenic emissions are also
430 seasonal which contributes to the seasonal change in O₃ concentrations (Pacifico et al., 2012;Young et al., 2009),
431 and dry deposition, driven by plant productivity also has a strong seasonal component. How the seasonality of
432 ground level O₃ changes in the future will depend on how these multiple different drivers change and interact.
433 Modelling studies such as Dentener et al. (2006) and Young et al. (2013) suggest that anthropogenic emissions
434 will be the main factor controlling the evolution of future O₃ concentrations, and in the recent study of Young et
435 al., (2013) most scenarios suggest reduced O₃ burden in the future as a result predominantly of reduced precursor
436 emissions. Seasonally, the O₃ concentrations used in the simulations in this study show increased O₃ levels in
437 winter and in some regions in autumn and spring in 2050 compared to present day, this may be due to reduced
438 titration of O₃ by NO as a result of reduced NO_x emissions in the future (Royal Society, 2008). Summer O₃
439 concentrations are lower in 2050 however, compared to 2001. Our simulations use a fixed climate, so we do not
440 include the effect of climate change on shifting plant phenology. Therefore, our results may underestimate plant
441 O₃ damage, since if the growing season started earlier or finished later, plants in some regions would be exposed
442 to higher O₃ concentrations.

Commented [ORJ25]: RC2 5)

443
444



445
 446 **Figure 1.** Regional time series of canopy height O₃ (ppb) forcing from EMEP a) to c), and d) global atmospheric
 447 CO₂ (ppm) concentration (this does not vary regionally; black dots show data points, the black line shows
 448 interpolated points). Each panel for the O₃ forcing shows the regional annual average (woody PFTs, black solid
 449 line; herbaceous PFTs, black dashed line) and the annual maximum O₃ concentration above: woody PFTs (red)
 450 and herbaceous PFTs (blue).

451
 452 **2.4.2 Spin up and factorial experiments**

453
 454 JULES was spun-up by recycling the climate from the early part of the twentieth century (1901 to 1920) using
 455 atmospheric CO₂ (296.1 ppm) and O₃ concentrations from 1901 (Fig. S3 & Fig. S4). Model spin-up was 2000
 456 years by which point the carbon pools and fluxes were in steady state with zero mean net land – atmosphere CO₂
 457 flux. We performed the following transient simulations for the period 1901 to 2050 with continued recycling of
 458 the climate as used in the spin-up, for both high and low plant O₃ sensitivities:

- 459 • **O3** : Fixed 1901 CO₂, Varying O₃
- 460 • **CO2** : Varying CO₂, Fixed 1901 O₃
- 461 • **CO2 + O3** : Varying CO₂, Varying O₃

462
 463
 464 We use these simulations to investigate the direct effects of changing atmospheric CO₂ and O₃ concentrations,
 465 individually and combined, on plant physiology through the twentieth century and into the future, specifically
 466 over three time periods: historical (1901-2001), future (2001-2050) and over the full time series (1901-2050). See
 467 [more details in the SI section S6 for calculation of the effects due to O₃, CO₂ and O₃ + CO₂. We also use paired](#)
 468 [t-test to determine statistically significant differences between the different \(high and low\) plant O₃ sensitivities.](#)

Commented [ORJ26]: RC1 13)

469
 470 **2.4.3 Evaluation**

471 To evaluate our JULES simulations we compare mean GPP from 1991 to 2001 for each of the JULES scenarios
472 and both high and low plant O₃ sensitivities against the observation based globally extrapolated Flux Network
473 model tree ensemble (MTE) (Jung et al., 2011). We use paired t-test to determine statistically significant
474 differences in the mean responses.

Commented [ORJ27]: RC2 3)

476 3 Results

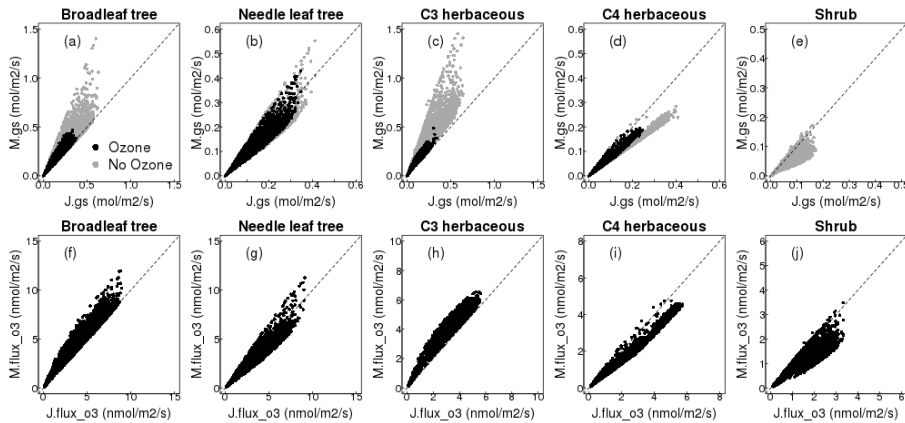
478 3.1 Impact of g_s model formulation

479 The impact of g_s model on simulated g_s is shown for the wet site (Fig. 2). For the broadleaf tree and C₃ herbaceous
480 PFT, the MEDedlyn-g_s model simulates a significantly larger conductance compared to the JACaeobs-g_s model.
481 In other words, with the MEDedlyn-g_s model these two PFTs are parameterised with a less conservative water use
482 strategy, which, for the grid point shown in Fig. 2 used in the simulation, increased the annual mean leaf-level
483 water use by 3522% (±29%) and 45% (±32%), respectively. In contrast, the needle leaf tree, C₄ herbaceous and
484 shrub PFTs are parameterised with a more conservative water use strategy with the MEDedlyn-g_s model, and the
485 mean annual g_s was decreased by 136% (±12%), -2732% (±10%) and 3641% (±13%), respectively, compared
486 to the JACaeobs-g_s model. This comparison was also done for a dry site, and similar results were found (Fig. S6),
487 suggesting these results are representative across the domain. The effect of g_s formulation model on simulated
488 photosynthesis was much smaller because of the lower sensitivity of the limiting rates of photosynthesis to
489 changes in c_i in the model compared to the effect of the same change in c_i on modelled g_c (Fig. S7 & S8). Changes
490 in leaf-level g_s impact the partitioning of simulated energy fluxes. In general, increased g_s results in increased
491 latent heat and thus decreased sensible heat flux, and vice versa where g_s is decreased (Fig. S7 & S8). Also shown
492 is the effect of the MEDedlyn-g_s model on O₃ flux into the leaf (Fig. 2 and Fig. S6, bottom panels). For the
493 broadleaf tree and C₃ herbaceous PFT, the MEDedlyn model simulates a larger conductance and therefore a
494 greater flux of O₃ through stomata compared to JACaeobs, and this is indicative of the potential for greater
495 reductions in photosynthesis (Fig. S7 & S8). The reverse is seen for the needle leaf tree, C₄ herbaceous and shrub
496 PFTs. See SI section S4 for site level evaluation of the seasonal cycles of latent and sensible heat with both JAC
497 and MED models compared to FLUXNET observations.

Commented [ORJ28]: RC1 10)

Commented [ORJ29]: RC1 11)

499



500
 501 **Figure 2.** Comparison of simulated g_s with the MEDeDlyn *et al.*, (2011) (y axis) versus the JACaeobs (1994)
 502 formulation (x axis) currently used in JULES for all five JULES PFTs at one grid point (lat: 48.25; lon: 5.25)
 503 shown are hourly values for the year 2000 (see SI section S3 for further details). Shown are s for stomatal
 504 conductance (g_s , top row) and the flux of O_3 through the stomata (flux_o3, bottom row).

505
 506 **3.2 Evaluation of the JULES O_3 model**
 507 For all JULES scenarios similar spatial patterns of GPP are simulated compared to MTE (Fig. 3 and Fig. S10).
 508 MTE estimates a mean GPP for present day in Europe of $938 \text{ gC m}^{-2} \text{ yr}^{-1}$ (Fig. 3). JULES tends to under-predict
 509 GPP relative to the MTE product, estimates of GPP from JULES with both transient CO_2 and O_3 give a mean
 510 across Europe of $813 \text{ gC m}^{-2} \text{ yr}^{-1}$ (high plant O_3 sensitivity) to $881 \text{ gC m}^{-2} \text{ yr}^{-1}$ (low plant O_3 sensitivity), both of
 511 which are significantly different to the MTE product ($t=27, d.f.=5750, p<2.2e^{-16}$ (high); $t=4.3, d.f.=5750, p<1.5e^{-05}$
 512 (low); Fig. 3). Forcing with CO_2 alone (fixed 1901 O_3) gives a mean GPP across Europe of 900 to 923 gC m^{-2}
 513 yr^{-1} (high and low plant O_3 sensitivity respectively), and O_3 alone (without the protective effect of CO_2) reduces
 514 estimated GPP to 732 to $799 \text{ gC m}^{-2} \text{ yr}^{-1}$ (Fig. S10). At latitudes $>45^\circ N$ JULES has a tendency to under-predict
 515 MTE-GPP, and at latitudes $<45^\circ N$ JULES tends to over-predict MTE-GPP (Fig. S11). These regional differences
 516 are highlighted in Fig. S12, where in the Mediterranean region, JULES tends to over-predict MTE-GPP, so
 517 simulations with O_3 reduce the simulated GPP bringing it closer to MTE. In the temperate region however, JULES
 518 tends to under-estimate MTE-GPP, so the addition of O_3 reduces simulated GPP further (Fig. S12). In the boreal
 519 region, JULES under-predicts GPP, but to a lesser extent than in the temperate region, and the addition of O_3 has
 520 less impact on reducing the GPP further (Fig. S12).

521

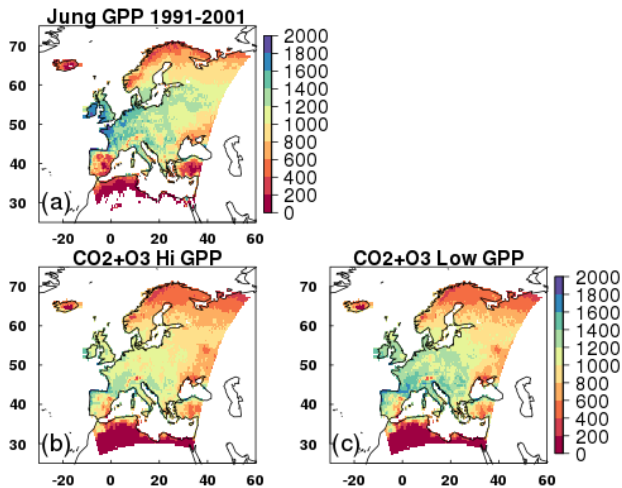


Figure 3. Mean GPP ($\text{g C m}^{-2} \text{ yr}^{-1}$) from 1991 to 2001 for a) the observationally based globally extrapolated Flux Network model tree ensemble (MTE) (Jung *et al.*, 2011); b, c) model simulations with transient CO_2 and transient O_3 , high and low plant O_3 sensitivity respectively.

Commented [ORJ30]: RC2 3)

3.3 European simulations - Historical Period: 1901-2001

Over the historical period (1901-2001), the physiological effect of O_3 reduced GPP (-3% to -9%) for the low and high plant O_3 sensitivity parameterizations, respectively (Table 1). The difference in plant O_3 sensitivity was significant ($t=102.2$, $df=6270$, $p<2.2e^{-16}$). Figure 43 highlights regional variations, however, where simulated reductions in GPP are up to 20% across large areas of Europe, and up to 30% in some Mediterranean regions under the high plant O_3 sensitivity. Some Boreal and Mediterranean regions show small increases in increased GPP over this period, associated with O_3 induced stomatal closure enhancing water availability in these drier regions (Fig. 54). This allows for greater enhancing stomatal conductance later in the year when soil moisture may otherwise have been limiting to growth (up to 10%, Fig. 5), and therefore higher GPP, but these regions comprise only a small area of the entire domain. Indeed, over much of the Europe, O_3 -induced stomatal closure led to reduced g_s (up to 20%) across large areas of temperate Europe and the Mediterranean, and even greater reductions in some smaller regions of southern Mediterranean (Fig. 65), and these are not associated with notable significant increases in soil moisture availability (Fig. 54), resulting in depressed GPP over much of Europe as described above. Under the low plant O_3 sensitivity, similar spatial patterns occur, but the magnitude of GPP change (up to -10% across much of Europe) and g_s change (-5% to -10%) are lower compared to the high sensitivity. Over the twentieth century the land carbon sink is significantly-suppressed (-2% to -6%, Table 1). Large regional variation is shown in Figure 43, with temperate and Mediterranean Europe seeing a large reduction in land carbon storage, particularly under the high plant O_3 sensitivity (up to -15%). Combined, the physiological

Commented [ORJ31]: RC1 13)

Commented [ORJ32]: RC1 12)

547 response to changing CO₂ and O₃ concentrations results in a net loss of land carbon over the twentieth century
548 under the high plant O₃ sensitivity (-2%, Table 1), dominated by loss of soil carbon (Table S32). This reflects the
549 large increases in tropospheric O₃ concentration observed over this period (Fig. 1). Under the low plant O₃
550 sensitivity, the land carbon sink has started to recover by 2001 (+1.5%) owing to the recovery of the soil carbon
551 pool beyond 1901 values over this period (Table S32).

552
553 To gain perspective on the magnitude of the O₃ induced flux of carbon from the land to the atmosphere we relate
554 changes in total land carbon to carbon emissions from fossil fuel combustion and cement production for the EU-
555 28-plus countries from the data of Boden et al. (2013). We recognise that our simulation domain is slightly larger
556 than the EU28-plus as it includes a small area of western Russia so direct comparisons cannot be made, but this
557 still provides a useful measure of the size of the carbon flux. For the period 1970 to 1979 the simulated loss of
558 carbon from the European terrestrial biosphere due to O₃ effects on vegetation physiology was on average 1.32
559 Pg C (high vegetation sensitivity) and 0.71 Pg C (low vegetation sensitivity) (Table 2). This O₃ induced reduced
560 C uptake of the land surface is equivalent to around 8% to 16% of the emissions of carbon from fossil fuel
561 combustion and cement production over the same period for the EU28-plus countries (Table 2). Currently the
562 emissions data availability goes up to 2011, so over the last observable decade (2002 to 2011) this land carbon
563 loss has declined but is still equivalent to 2% to 4% of the emissions of carbon from fossil fuels and cement
564 production for the EU28-plus countries (Table 2). Therefore, the indirect O₃ effect on the land carbon sink
565 potentially represents a significant additional source of anthropogenic carbon.

566 3.4.3 European simulations - Future Period: 2001-2050

567
568
569 Over the 2001 to 2050 period, region-wide GPP with O₃ only changing increased marginally (+0.1% to +0.2%,
570 high and low plant O₃ sensitivity, Table 1, with a significant difference between the two plant O₃ sensitivities
571 ($t=57, df=6270, p<2.2e^{-16}$), although with large spatial variability (Fig. 43g & h). This reflects changes in
572 tropospheric O₃ concentration as emission control policies reduce O₃ concentrations. Figures S34 and S45 show
573 that despite decreased tropospheric O₃ concentrations by 2050 in summer compared to 2001 levels, all regions are
574 exposed to an increase in O₃ over the wintertime, and some regions of Europe, particularly
575 temperate/Mediterranean experience increases in O₃ concentration in spring and autumn. Therefore, although
576 increased GPP (dominantly 10%, but up to 20% in some areas) on 2001 levels is simulated across large areas of
577 Europe, decreases of up to 21% are simulated in some areas of the Mediterranean, up to 15% in some areas of the
578 boreal region and up to 27% in the temperate zone (Fig. 4g & h). When O₃ and CO₂ effects are combined,
579 simulated GPP increases (+15% to +18%, high/low plant O₃ sensitivities respectively, Table 1). This increase is
580 greater than the enhancement simulated when CO₂ affects plant growth independently, because additional O₃
581 induced stomatal closure increases soil water availability in some regions, which enhances growth more in the O₃
582 and CO₂ simulations, compared to the CO₂ only run. Nevertheless, although the percentage gain is larger, the
583 absolute value of GPP by 2050 remains lower compared to GPP with CO₂ only changing (Table S43).

584
585 Despite small increases in GPP in the O₃-only simulation, the land carbon sink continues to decline from 2001
586 levels (-0.7% to -1.6%, low and high plant O₃ sensitivity respectively, Table 1). This is because the soil and

Commented [ORJ33]: RC1 13)

587 vegetation carbon pools continue to lose carbon as they adjust slowly to small changes in input (GPP), i.e. the soil
588 carbon pool is not in equilibrium in 2001, and is declining in response to reduced litter input as a result of 20th C
589 O₃ impacts on GPP. Nevertheless, the negative effect of O₃ on the future land sink is markedly reduced relative
590 to the historical period. Figure 4e & f however highlights regional differences. Boreal regions and parts of central
591 Europe see minimal O₃ damage, whereas some areas of southern and northern Europe see further losses of up to
592 8% on 2001 levels. The combined O₃ and CO₂ effects are dominated by the physiological effects of changing
593 CO₂, with land carbon sink increases of up to 7% (Table 1).

Commented [ORJ34]: RC1 16)

594 **3.5.4 European simulations - Anthropocene: 1901-2050**

595
596
597 Over the Anthropocene, O₃ reduces GPP (-4% to -9%, with a significant difference between the low and high
598 plant O₃ sensitivity ($t=95, d.f.=6270, p<2.2e^{-16}$)) and land carbon storage (-3% to -7%, Table 1, Fig. S139).
599 Regionally, O₃ damage is lowest in the boreal zone, GPP decreases are largely between 5% to 8% / 2% to 4% for
600 the high/low plant O₃ sensitivity respectively, with large areas minimally affected by O₃ damage (Figure 76),
601 consistent with lower *g_s* of needle leaf trees that dominate this region, and so lower O₃ uptake (Fig. S140 & S154).
602 In the temperate region, O₃ damage is extensive with reductions in GPP dominantly from 10% to 15% for the low
603 and high plant O₃ sensitivity respectively. Across significant areas of this region reductions in GPP are up to 20%
604 under high plant O₃ sensitivity (Figure 76). In the Mediterranean region, O₃ damage reduces GPP by 5% to 15%
605 / 3% to 6% for the high/low plant O₃ sensitivity respectively, with some areas seeing greater losses of up to 20%
606 under the high plant O₃ sensitivity, but this is less extensive than that seen in the temperate zone (Figure 76). In
607 these drier regions, O₃ induced stomatal closure can increase available soil moisture (Fig. S140 & S154).

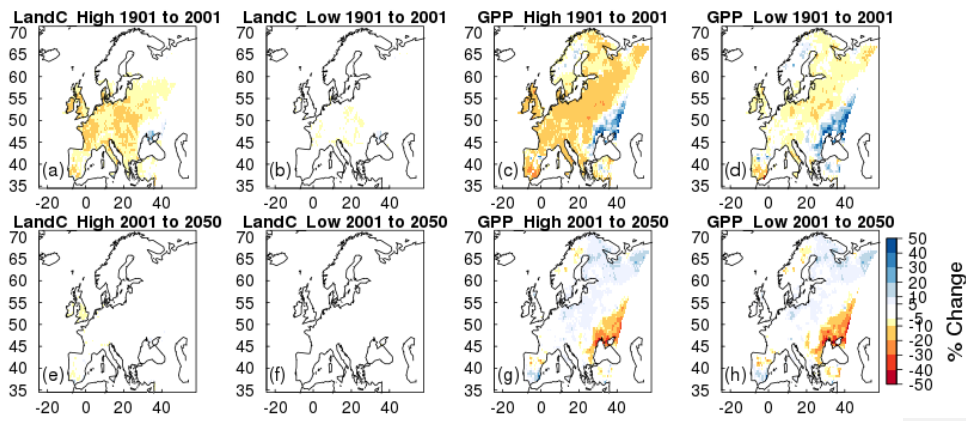
Commented [ORJ35]: RC1 13)

608
609 Varying CO₂ and O₃ together shows that CO₂ induced stomatal closure can help alleviate O₃ damage by reducing
610 the uptake of O₃ (Table S65). In these simulations, CO₂-induced stomatal closure was found to offset O₃-
611 suppression of GPP, such that GPP by 2050 is 3% to 7% lower due to O₃ exposure, rather than 4% to 9% lower
612 in the absence of increasing CO₂ (Table S65). Figure 6 shows this spatially, O₃ damage is reduced when the effect
613 of atmospheric CO₂ on stomatal closure is accounted for, however despite this, the land carbon sink and GPP
614 remain significantly reduced due to O₃ exposure.

Commented [ORJ36]: RC1 2)

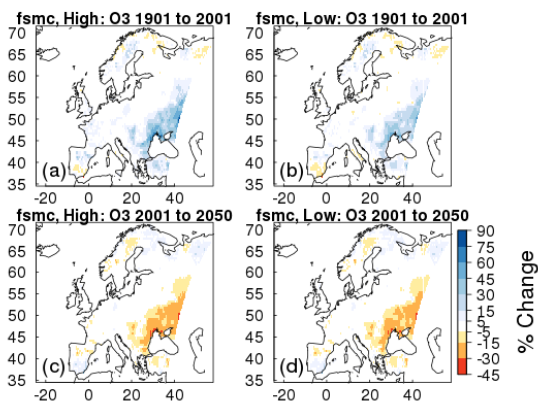
615
616 Over the Anthropocene, changing O₃ and CO₂ in tandem results in an increase in European land carbon uptake
617 (+5% to +9%), and an increase in GPP (+20% to +23%) by 2050 for the high and low plant O₃ sensitivity,
618 respectively (Table 1). Nevertheless, despite this increase there remains a large negative impact of O₃ on the
619 European land carbon sink (Fig. S139). By 2050 the simulated enhancement of land carbon and GPP in response
620 to elevated CO₂ alone is reduced by 3% to 6% (land carbon) and 4% to 9% (GPP) for the low and high plant O₃
621 sensitivity respectively, when O₃ is also accounted for (Table 1). This is a large significant reduction in the ability
622 of the European terrestrial biosphere to sequester carbon.

623



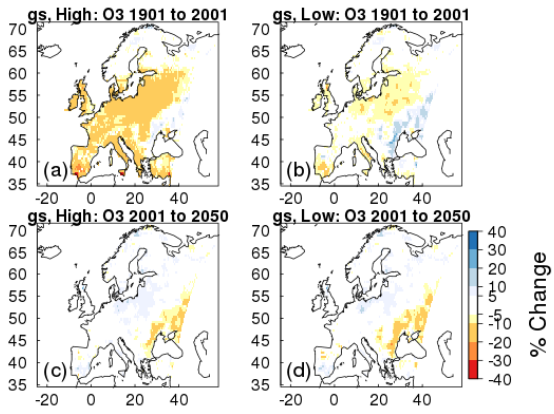
624

625 **Figure 43.** Simulated percentage change in total carbon stocks (Land C) and gross primary productivity (GPP)
 626 due to O₃ effects at fixed pre-industrial atmospheric CO₂ concentration. Changes are shown for the periods 1901
 627 to 2001, and 2001 to 2050 for the high and low plant O₃ sensitivity.
 628



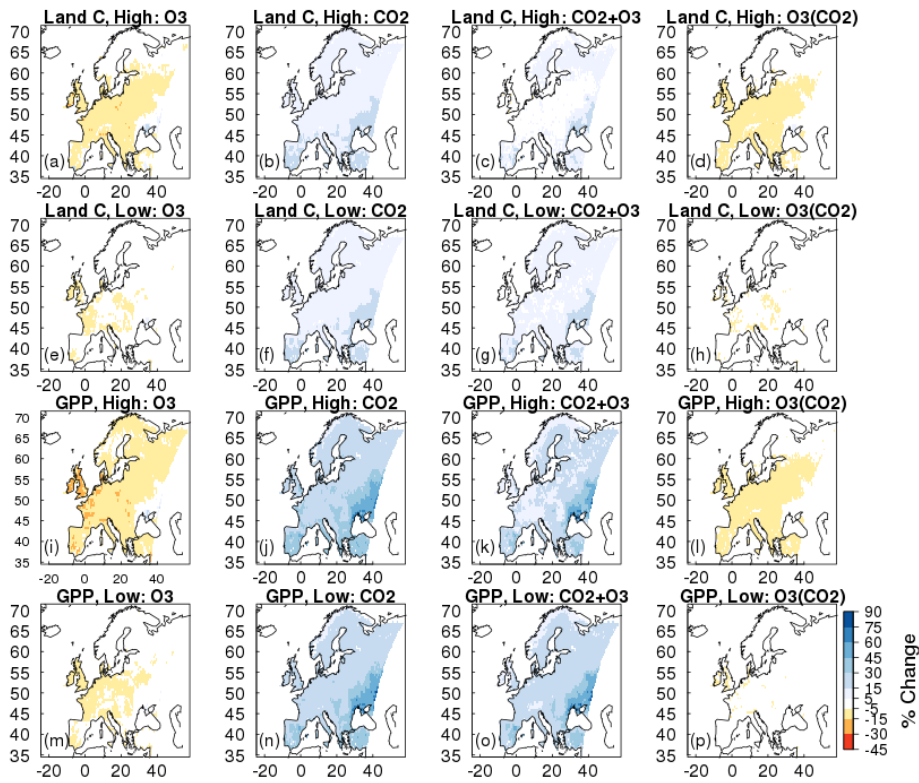
629

630 **Figure 54.** Simulated percentage change in plant available soil moisture (*fsmc*) due to O₃ effects at fixed pre-
 631 industrial atmospheric CO₂ concentration. Changes are shown for the periods 1901 to 2001, and 2001 to 2050 for
 632 the high and low plant O₃ sensitivity.
 633



634

635 **Figure 6.5.** Simulated percentage change in stomatal conductance (g_s) due to O_3 effects at fixed pre-industrial
 636 atmospheric CO_2 concentration. Changes are shown for the periods 1901 to 2001, and 2001 to 2050 for the high
 637 and low plant O_3 sensitivity.
 638



639

640 **Figure 76.** Simulated percentage change in total carbon stocks (Land C) and gross primary productivity (GPP)
 641 due to i) (a, e, i, m) O₃ effects at fixed pre-industrial atmospheric CO₂ concentration (O₃), ii) (b, f, j, n) CO₂
 642 fertilisation at fixed pre-industrial O₃ concentration (CO₂), iii) (c, g, k, o) the interaction between O₃ and CO₂
 643 effects (CO₂ + O₃) iv) (d, h, l, p) O₃ effects with changing atmospheric CO₂ concentration (i.e. O₃ damage
 644 accounting for the effect of CO₂ induced stomatal closure; O₃(CO₂)). Changes are depicted for the periods 1901
 645 to 2050 for high and lower ozone plant sensitivity.

646

647

648

649

650

651

652

	High Plant O ₃ Sensitivity					
	1901 - 2001		2001 - 2050		1901 - 2050	
	GPP (Pg C yr ⁻¹)	Land C (Pg C)	GPP (Pg C yr ⁻¹)	Land C (Pg C)	GPP (Pg C yr ⁻¹)	Land C (Pg C)
Value in 1901:	9.05	167	-	-	9.05	167
Absolute Change:						
O ₃	-0.81	-9.21	0.01	-2.44	-0.80	-11.65
CO ₂	1.16	4.24	1.42	12.98	2.58	17.22
CO ₂ + O ₃	0.13	-3.28	1.66	11.11	1.79	7.83
% Change:						
O ₃	-8.95	-5.51	0.12	-1.55	-8.84	-6.98
CO ₂	12.82	2.54	13.91	7.58	28.51	10.31
CO ₂ + O ₃	1.44	-1.96	18.08	6.79	19.78	4.69
	Low Plant O ₃ Sensitivity					
	1901 - 2001		2001 - 2050		1901 - 2050	
	GPP (Pg C yr ⁻¹)	Land C (Pg C)	GPP (Pg C yr ⁻¹)	Land C (Pg C)	GPP (Pg C yr ⁻¹)	Land C (Pg C)
Value in 1901:	9.34	167.5	-	-	9.34	167.5
Absolute Change:						
O ₃	-0.30	-3.59	0.02	-1.07	-0.40	-4.66
CO ₂	1.15	6.43	1.35	13.14	2.50	19.57
CO ₂ + O ₃	0.65	2.50	1.50	12.35	2.15	14.85
% Change:						
O ₃	-3.21	-2.14	0.22	-0.65	-4.28	-2.78
CO ₂	12.31	3.84	12.87	7.55	26.77	11.68
CO ₂ + O ₃	6.96	1.49	15.02	7.26	23.02	8.87

653

654 **Table 1.** Simulated changes in the European land carbon cycle due to changing O₃ and CO₂ concentrations
655 (independently and together). Shown are changes in total carbon stocks (Land C) and gross primary productivity
656 (GPP), over three different periods (historical: 1901 to 2001, future: 2001 to 2050, and Anthropocene: 1901 to
657 2050). Absolute (top) and relative (bottom) differences are shown. For 2001 to 2050, please refer to Table S43
658 for the initial value for each run. See the SI for details of the estimation of the O₃ and CO₂ effects and their
659 interaction.

660

661

662

663

664

665

666

667

668

	Mean (Pg C)				
	1970-1979	1980-1989	1990-1999	2000-2009	2002-2011
Modelled O₃ effect on land C sink :					
Higher sensitivity	-1.32	-1.01	-0.97	-0.53	-0.50
Low sensitivity	-0.71	-0.58	-0.50	-0.29	-0.26
Sum of C emissions from fossil fuel combustion and cement production (Pg C)					
	8.39	8.63	12.26	12.83	12.75
C lost from O₃ effect as a % of fossil fuel and cement emissions (%):					
Higher sensitivity	-15.73	-11.70	-7.91	-4.13	-3.92
Low sensitivity	-8.46	-6.72	-4.08	-2.26	-2.04

670

671 **Table 2.** Simulated change in total land carbon due to O₃ damage with changing atmospheric CO₂ concentration
672 for the two vegetation sensitivities. The sum of carbon emissions for each decade from fossil fuel combustion and
673 cement production for the EU-28 countries plus Albania, Bosnia and Herzegovina, Iceland, Belarus, Serbia,
674 Moldova, Norway, Turkey, Ukraine, Switzerland and Macedonia (EU28-plus) are shown, the data is from Boden
675 *et al.*, 2013. The simulated change in land carbon as a result of O₃ damage is depicted as a percentage of the EU28-
676 plus emissions to demonstrate the magnitude of the additional source of carbon to the atmosphere from plant O₃
677 damage.

678

679 4 Discussion

680

681 4.1 Comparison of *g_s* models

682

683 Comparison of the new *g_s* model implemented in this study (MEDedlyn *et al.*, 2014) with the *g_s* model currently
684 used as standard in JULES (JACaeobs-1994) revealed large differences in leaf-level *g_s* for each PFT, principally
685 as a result of the data-based parameterisation of the new model. Leaf-level water use increased for the broadleaf
686 tree and C₃ herbaceous PFTs using the MEDedlyn-*g_s* model compared to JACaeobs, but decreased for the needle
687 leaf tree, C₄ herbaceous and shrub PFTs which displayed a more conservative water use strategy compared to the
688 Jacobs parameterisation. These changes are in line with the work of De Kauwe *et al.* (2015) who found a reduction
689 in annual transpiration for evergreen needle leaf, tundra and C₄ grass regions when implementing the Medlyn *g_s*
690 model into the Australian land surface scheme CABLE. Changes in leaf-level *g_s* in this study resulted in
691 differences in latent and sensible heat fluxes. Changes in the partitioning of energy fluxes at the land surface could
692 potentially have consequences for the intensity of heatwaves (Cruz *et al.*, 2010; Kala *et al.*, 2016), runoff (Betts *et al.*,
693 2007; Gedney *et al.*, 2006) and rainfall patterns (de Arellano *et al.*, 2012), although fully coupled simulations
694 would be necessary to detect these effects. The differences in effect of the *g_s* model on simulated *g_s* stomatal
695 conductance led to differences in the uptake of O₃ between the two *g_s* models because the leaf-level rate of *g_s*
696 is the predominant determinant of the flux of O₃ through stomata. Higher O₃ uptake is indicative of greater damage.
697 Therefore, given that C₃ herbaceous vegetation is the dominant land cover class across the European domain used

698 in this study, this suggests a greater O₃ impact for Europe ~~would be simulated with the MED edlyn-g_s~~
699 ~~model compared to JAC, and that studies using the Jacobs g_s formulation may underestimate the O₃ impact for~~
700 ~~Europe.~~

Commented [ORJ37]: RC2 3)

701 **4.2 Lower than expected O₃ damage?**

702 We compare results from the present study to values found in literature. The Wittig et al. (2007) meta-analysis of
703 temperate and boreal tree species showed future concentrations of O₃ predicted for 2050 significantly reduced leaf
704 level light saturated net photosynthetic uptake (-19%, range: -3% to -28%) and g_s (-10%, range: +5% to -23%) in
705 both broadleaf and needle-leaf tree species. In the Feng et al. (2008) meta-analysis of wheat, projected O₃
706 concentrations for the future reduced aboveground biomass (-18%, CI -13% to -24%), photosynthetic rate (-20%)
707 and g_s (-22%). One of few long-term field-based O₃ exposure studies (AspenFACE) showed that after 11 years of
708 exposing mature trees to elevated O₃ concentrations, O₃ decreased ecosystem carbon content (-9%), and decreased
709 NPP (-10%), although the O₃ effect decreased through time (Falhelm et al., 2014). GPP was reduced (-12% to
710 -19%) at two Mediterranean ecosystems (dominated by either *Pinus* species or *Citrus* species) studied by Fares et
711 al. (2013). Biomass of mature beech trees was reduced (-44%) after 8 years of exposure to elevated O₃ (Matyssek
712 et al., 2010a). After 5 years of O₃ exposure in a semi-natural grassland, annual biomass production was reduced
713 (-23%), and in a Mediterranean annual pasture O₃ exposure significantly reduced total aboveground biomass (up
714 to -25%) (Calvete-Sogo et al., 2014). Results from the present study suggest projected O₃ concentrations for 2050
715 will reduce mean GPP for Europe (-4% to -9%), NPP (-6% to -11%), total carbon content (-3% to -7%) and g_s (-
716 4% to -9%). Using GPP as a proxy for A_{max} (these variables are not identical but they are related), our mean GPP
717 and g_s estimates fall within the range given by the meta-analysis of Wittig et al. (2007). The remaining studies are
718 not meta-analyses, so are site- and species-specific, our estimates appear to compare more conservatively with
719 these, however these are a mean value for Europe and spatially our estimates show greater variability.

720
721 The impact of O₃ on present day European GPP simulated in this study is slightly lower compared to previous
722 ~~modelled estimates studies~~. Our estimates suggest present day O₃ reduced GPP by 3% to 9% on average across
723 Europe and NPP by 5% to 11% (Table S3). Anav et al. (2011) simulated a 22% reduction of GPP across Europe
724 for 2002 using the ORCHIDEE model. Present day O₃ exposure reduced GPP by 10% to 25% in Europe, and
725 10.8% globally in the study by Lombardozzi et al. (2015) using the Community land model (CLM). O₃ reduced
726 NPP by 11.2% in Europe from 1989 to 1995 using the Terrestrial Ecosystem Model (TEM) (Felzer et al., 2005).
727 Globally, concentrations of O₃ predicted for 2100 reduced GPP by 14% to 23% using a former parameterisation
728 of O₃ sensitivity in JULES (Sitch et al., 2007). The recent study by Franz et al. (2017) showed mean GPP declined
729 by 4.7% over the period 2001 to 2010 using the OCN model over the same European domain used in this study.
730 These ~~similar similarly 'lower than expected'~~ results are likely the result of using the same domain, and, more
731 importantly, O₃ forcing produced by the same model (EMEP MSC-W).

733 **4.3 Impacts of O₃ at the land surface**

734
735 In this study, O₃ has a detrimental effect on the size of the land carbon sink for Europe. This is primarily through
736 a decrease in the size of the soil carbon pool as a result of reduced litter input to the soil, consistent with reduced
737 GPP/NPP. Field studies show that in some regions of Europe, soil carbon stocks are decreasing (Bellamy et al.,

738 2005;Capriel, 2013;Heikkinen et al., 2013;Sleutel et al., 2003). The study of Bellamy et al. (2005), for example,
739 showed that carbon was lost from soils across England and Wales between 1978 to 2003 at a mean rate of 0.6%
740 per year with little effect of land use on the rate of carbon loss, suggesting a possible link to climate change. It is
741 understood that climate change is likely to affect soil carbon turnover. Increased temperatures increase microbial
742 decomposition activity in the soil, and therefore increase carbon losses through higher rates of respiration (Cox et
743 al., 2000;Friedlingstein et al., 2006;Jones et al., 2003). However, some studies have found that O₃ can decrease
744 soil carbon content. Talhelm et al. (2014), for example, found O₃ reduced carbon content in near surface mineral
745 soil of forest soils exposed to 11 years of O₃ fumigation. Hofmockel et al. (2011) found elevated O₃ reduced the
746 carbon content in more stable soil organic matter pools, and Loya et al. (2003) showed that the fraction of soil
747 carbon formed in forest soils over a 4 year experimental period when fumigated with both CO₂ and O₃ was reduced
748 by 51% compared to the soil fumigated with CO₂ alone. It is agreed that amongst other factors that change with
749 O₃ exposure such as litter quality and composition, reduced litter quantity also has significant detrimental
750 consequences for soil carbon stocks (Andersen, 2003;Lindroth, 2010;Loya et al., 2003). Results from this study
751 therefore suggest that increasing tropospheric O₃ may be a contributing factor to the declining soil carbon stocks
752 observed across Europe as a result of reduced litter input to the soil carbon pool consistent with reduced NPP.

753
754 We acknowledge, however, that our model simulations do not include coupling of Nitrogen and Carbon cycles,
755 or land management practices. Although we include a representation of agricultural regions through the model
756 calibration against the wheat O₃ sensitivity function (CLRTAP, 2017), wheat is known to be one of the most O₃
757 sensitive crop species. As with all uncoupled modelling studies, a change in g_s and flux will impact the O₃
758 concentration itself. Therefore adopting the Medlyn formulation with a higher g_s and subsequently higher O₃ flux
759 for broadleaf and C₃ PFTs (Fig 2) would lead to reduced O₃ concentration, which in turn would act to dampen the
760 effect of higher g_s on O₃ flux. Essentially this study provides an 'upper bound' as in the high plant O₃ sensitivity
761 scenario, all C₃/C₄ fractional cover uses the wheat O₃ sensitivity. Additionally, this version of JULES does not
762 have a crop module; it has no land management practices such as harvesting, ploughing or crop rotation –
763 processes which may have counteracting effects on the land carbon sink. Further, without a coupled Carbon and
764 Nitrogen cycle, it is likely that the CO₂ fertilisation response of GPP and the land carbon sink is over estimated in
765 some regions of our simulations since nitrogen availability limits terrestrial carbon sequestration of natural
766 ecosystems in the temperate and boreal zone (Zaehle, 2013). This would have consequences for our modelled O₃
767 impact, particularly into the future where the large CO₂ fertilisation effect was responsible for partly offsetting
768 the negative impact of O₃. Although in our simulations a high fraction of land cover is agricultural which we
769 assume would be optimally fertilised. Nevertheless, we emphasise that this study provides a sensitivity assessment
770 of the impact of plant O₃ damage on GPP and the land carbon sink.

771
772 Another caveat we fully acknowledge is that at the leaf-level JULES is parameterised to reduce g_s with O₃
773 exposure. Whilst this response is commonly observed (Wittig et al., 2007;Ainsworth et al., 2012), there is evidence
774 to suggest that O₃ impairs stomata in some species, making them non-responsive to environmental stimuli (Hayes
775 et al., 2012;Hoshika et al., 2012a;Mills et al., 2009;Paoletti and Grulke, 2010). In drought conditions the
776 mechanism is thought to involve O₃ stimulated ethylene production which interferes with the stomatal response
777 to ABA signalling (Wilkinson and Davies, 2009;Wilkinson and Davies, 2010). Such stomatal sluggishness can

Commented [ORJ38]: RC2 minor comment 16.

778 result in higher O₃ uptake and injury, increased water-loss, and therefore greater vulnerability to environmental
779 stresses (Mills et al., 2016). McLaughlin (2007a;2007b) and Sun et al. (2012) provide evidence of increased
780 transpiration and reduced streamflow in forests at the regional scale in response to ambient levels of O₃, and
781 suggest this could increase the frequency and severity of droughts. (Hoshika et al., 2012b) [Hoshika et al 2012](#)
782 [however found that despite sluggish stomatal control in O₃ exposed trees, whole tree water use was lower in these](#)
783 [trees because of lower gas exchange and premature leaf shedding of injured leaves.](#) To our knowledge, the study
784 of Hoshika et al. (2015) is the first to include an explicit representation of sluggish stomatal control in a land-
785 atmosphere model, they show that sluggish stomatal behaviour has [significant](#) implications for carbon and water
786 cycling in ecosystems. However, it is by no means a ubiquitous response, and it is not fully understood which
787 species respond this way and under what conditions (Mills et al., 2016; Wittig et al., 2007). Nevertheless, this
788 remains an important area of future work.

789
790 [The calculation of O₃ deposition in the EMEP model uses the stomatal conductance formulation presented in](#)
791 [Emberson et al. \(2000;2001\), which depends on temperature, light, humidity and soil moisture \(commonly](#)
792 [referred to as DO₃SE\). Because we link two different model systems, the g_s values in the EMEP model differ from](#)
793 [those obtained using the Medlyn formulation. We acknowledge this inconsistency as a caveat of our study,](#)
794 [however comparison of g_{max} \(maximum g_s\) values from both models \(EMEP and JULES\) suggests the](#)
795 [differences are small for deciduous forest \(EMEP 150-200, JULES ~180, all units in mmole O₃/m² \(PLA\)/s\), and](#)
796 [C₃/C₄ crops \(EMEP 270-300, JULES ~260-390 – the dominant land cover in our simulations\), but are larger for](#)
797 [coniferous forest \(EMEP 140-200, JULES ~60-70\) and shrubs \(EMEP 60-200, JULES 360-390\). The role of](#)
798 [EMEP in this study is not to provide g_s, however, but to provide O₃ at the top of the vegetation canopy. The main](#)
799 [driver of such O₃ levels is the regional-scale production and transport of O₃, and the main impact of g_s is in](#)
800 [affecting the vertical O₃ gradients just above the plant canopy. Differences in g_s are known to have minimal impact](#)
801 [on canopy-top O₃ for trees, mainly due to the efficient turbulent mixing above tall canopies, but also due to non-](#)
802 [stomatal sink processes. For shorter vegetation, substantial O₃ gradients, driven by deposition, occur in the lowest](#)
803 [10s of metres of the atmosphere, and stomatal sinks \(as given by g_s\) can have a significant role. However,](#)
804 [calculations of such gradients made with the EMEP model for CLRTAP \(2017\) showed that differences amounted](#)
805 [to only ca. 10% when comparing O₃ concentrations at 1m height above high-g_s crops compared to moderate-g_s](#)
806 [\(g_{max} = 450 and 270 mmole O₃/m² \(PLA\)/s respectively\), therefore this uncertainty is small.](#)

Commented [ORJ39]: RC2 4)

807
808 [These offline simulations show the sensitivity of GPP and the land carbon sink to tropospheric O₃, suggesting that](#)
809 [O₃ is an important predictor of future GPP and the land carbon store across Europe. There are uncertainties in our](#)
810 [estimates however from the use of uncoupled tropospheric chemistry, meteorology and stomatal function. For](#)
811 [example, increased frequency of drought in the future would reduce stomatal conductance \(assuming no sluggish](#)
812 [stomatal response\) and thus O₃ uptake. Since our offline simulations do not include this feedback it is possible the](#)
813 [O₃ effect is over estimated here. Given the complexity of potential interactions and feedbacks it remains difficult](#)
814 [to diagnose the importance of individual factors \(e.g. the direct physiological response\) in a fully coupled](#)
815 [simulation. Once the importance of a process is demonstrated offline, it provides evidence of the need to](#)
816 [incorporate such process in coupled regional and global simulations.](#)

Commented [ORJ40]: RC1 2)

Commented [ORJ41]: RC2 1)

818 4.4 O₃ as a missing component of carbon cycle assessments?

819
820 Comprehensive analyses of the European carbon balance suggest a ~~large significant~~ biogenic carbon sink
821 (Janssens et al., 2003;Luyssaert et al., 2012;Schulze et al., 2009). However, estimates are hampered by large
822 uncertainties in key components of the land carbon balance, such as estimates of soil carbon gains and losses
823 (Ciais et al., 2010;Janssens et al., 2003;Schulze et al., 2009;Schulze et al., 2010). We suggest that the effect of O₃
824 on plant physiology is a contributing factor to the decline in soil carbon stores observed across Europe, and as
825 such this O₃ effect is a missing component of European carbon cycle assessments. Over the Anthropocene, our
826 results show elevated O₃ concentrations reduce the amount of carbon that can be stored in the soil by 3% to 9%
827 (low and high plant O₃ sensitivity, respectively), which almost completely offsets the beneficial effects of CO₂
828 fertilisation on soil carbon storage under the high plant O₃ sensitivity . This would contribute to a ~~significant~~
829 change in the size of a key carbon sink for Europe, and is particularly important when we consider the evolution
830 of the land carbon sink into the future given the impact of O₃ on soil carbon sequestration and the high uncertainty
831 of future tropospheric O₃ concentrations. Schulze et al. (2009) and Luyssaert et al. (2012) extended their analysis
832 of the European carbon balance to include additional non-CO₂ greenhouse gases (CH₄ and N₂O). Both studies
833 found that emissions of these offset the biogenic carbon sink, reducing the climate mitigation potential of
834 European ecosystems. This highlights the importance of accounting for all fluxes and stores in carbon/greenhouse
835 gas balance assessments, of which O₃ and its indirect effect on the CO₂ flux via direct effects on plant physiology
836 is currently missing.

837 838 4.5 The interaction between O₃ and CO₂

839
840 We looked at the interaction between CO₂ and O₃ effects. Our results support the hypothesis that elevated
841 atmospheric CO₂ provides some protection against O₃ damage because of lower g_s that reduces uptake of O₃
842 through stomata (Harmens et al., 2007;Wittig et al., 2007). In the present study, reductions in GPP and the land
843 carbon store due to O₃ exposure were lower when simulated with concurrent changes in atmospheric CO₂. Despite
844 acclimation of photosynthesis after long-term exposure to elevated atmospheric CO₂ of field grown plants
845 (Ainsworth and Long, 2005;Medlyn et al., 1999), there is no evidence to suggest that g_s acclimates (Ainsworth et
846 al., 2003;Medlyn et al., 2001). This suggests the protective effect of elevated atmospheric CO₂ against O₃ damage
847 will be sustained in the long term. However, although meta-analysis suggest a general trend of reduced g_s with
848 elevated CO₂ (Ainsworth and Long, 2005;Medlyn et al., 1999), this is not a universal response. Stomatal responses
849 on exposure to elevated CO₂ with FACE treatment varied with genotype and growth stage in a fast-growing poplar
850 community (Bernacchi et al., 2003;Tricker et al., 2009). In other mature forest stands, limited stomatal response
851 to elevated CO₂ was observed after canopy closure (Ellsworth, 1999;Uddling et al., 2009). Also, some studies
852 found that stomatal responses to CO₂ were significant only under high atmospheric humidity (Cech et al.,
853 2003;Leuzinger and Körner, 2007;Wullschleger et al., 2002). These examples illustrate that stomatal responses to
854 elevated atmospheric CO₂ are not universal, and as such the protective effect of CO₂ against O₃ injury cannot be
855 assumed for all species, at all growth stages under wide ranging environmental conditions.

856 857 **5 Conclusion**

858
859 What is abundantly clear is that plant responses to both CO₂ and O₃ are complicated by a host of factors that are
860 only partly understood, and it remains difficult to identify general, global patterns given that effects of both gases
861 on plant communities and ecological interactions are highly context and species specific (Ainsworth and Long,
862 2005;Fuhrer et al., 2016;Matyssek et al., 2010b). This study quantifies the sensitivity of the land carbon sink for
863 Europe and GPP to changing concentrations of atmospheric CO₂ and O₃ from 1901 to 2050. We have used a state
864 of the art land surface model calibrated for European vegetation to give our best estimates of this sensitivity within
865 the limits of data availability to calibrate the model for O₃ sensitivity, current knowledge and model structure. In
866 summary, this study has shown that potential gains in terrestrial carbon sequestration over Europe resulting from
867 elevated CO₂ can be partially offset by concurrent rises in tropospheric O₃ over 1901-2050. Specifically, we have
868 shown that the negative effect of O₃ on the land carbon sink was greatest over the twentieth century, when O₃
869 concentrations increased rapidly from pre-industrial levels. Over this period soil carbon stocks were ~~significantly~~
870 diminished over agricultural areas, consistent with reduced NPP and litter input. This loss of soil carbon was
871 largely responsible for the decrease in the size of the land carbon sink over Europe. The O₃ effect on the land
872 carbon store and flux was reduced into the future as CO₂ concentration rose considerably and changes in O₃
873 concentration were less pronounced. However, there remained a large cumulative negative impact on the land
874 carbon sink for Europe by 2050. The interaction between the two gases was found to reduce O₃ injury owing to
875 reduced stomatal opening in elevated atmospheric CO₂. However, primary productivity and land carbon storage
876 remained ~~significantly~~ suppressed by 2050 due to plant O₃ damage. Expressed as a percentage of the emissions
877 from fossil fuel and cement production for the EU28-plus countries, the ~~additional~~ carbon emissions from O₃-
878 induced plant injury ~~are~~ is a potential significant additional source of anthropogenic carbon previously not
879 accounted for in carbon cycle assessments. Our results demonstrate the sensitivity of modelled terrestrial carbon
880 dynamics to the direct effect of tropospheric O₃ and its interaction with atmospheric CO₂ on plant physiology.
881 demonstrating this process is an important predictor of future GPP and trends in the land-carbon sink.
882 Nevertheless, this process remains largely unconsidered in regional and global climate model simulations that are
883 used to model carbon sources and sinks and carbon-climate feedbacks.

Commented [ORJ42]: RC2 1)

884
885
886 ~~, highlighting that such effects of O₃ on plant physiology significantly add to the uncertainty of future trends in~~
887 ~~the land carbon sink and climate carbon feedbacks. Given the potential to limit the climate mitigation effect of~~
888 ~~European terrestrial ecosystems, we suggest plant O₃ damage should be incorporated into carbon cycle~~
889 ~~assessments.~~

890 **Data availability**

891
892
893 The JULES model can be downloaded from the Met Office Science Repository Service
894 (<https://code.metoffice.gov.uk/trac/jules> - see here for a helpful how to [http://jules.jchmr.org/content/getting-](http://jules.jchmr.org/content/getting-started)
895 started). Model output data presented in this paper and the exact version of JULES with namelists are available
896 upon request from the corresponding author.
897

898 **Supplementary Information**

899

900 Supplementary_Information_Oliver_et_al.docx

901

902 **Competing Interests**

903 The authors declare that they have no conflict of interest

904

905 **Acknowledgements**

906

907 RJO and LMM were supported by the EU FP7 (ECLAIRE, 282910) and JWCRP (UKESM, NEC05816). This
908 work was also supported by EMEP under UNECE. SS and LMM acknowledge the support of the NERC
909 SAMBBA project (NE/J010057/1). The UK Met Office contribution was funded by BEIS under the Hadley Centre
910 Climate Programme (GA01101). GAF also acknowledges funding from the EU's Horizon 2020 research and
911 innovation programme (CRESCENDO, 641816). We also thank Magnuz Engardt of SMHI for providing the
912 RCA3 climate dataset.

913

914 **References**

915

- 916 [Ainsworth, E., and Long, S.: What have we learned from 15 years of free-air CO₂ enrichment \(FACE\)?](#)
917 [A meta-analytic review of the responses of photosynthesis, canopy properties and plant production](#)
918 [to rising CO₂, New Phytologist, 165, 351-372, 2005.](#)
919 Ainsworth, E. A., Davey, P. A., Hymus, G. J., Osborne, C. P., Rogers, A., Blum, H., Nosberger, J., and
920 Long, S. P.: Is stimulation of leaf photosynthesis by elevated carbon dioxide concentration
921 maintained in the long term? A test with *Lolium perenne* grown for 10 years at two nitrogen
922 fertilization levels under Free Air CO₂ Enrichment (FACE), *Plant, Cell and Environment*, 26, 705-714,
923 2003.
924 Ainsworth, E. A.: Rice production in a changing climate: a meta-analysis of responses to elevated
925 carbon dioxide and elevated ozone concentration, *Global Change Biology*, 14, 1642-1650,
926 [10.1111/j.1365-2486.2008.01594.x](#), 2008.
927 Ainsworth, E. A., Yendrek, C. R., Sitth, S., Collins, W. J., and Emberson, L. D.: The Effects of
928 Tropospheric Ozone on Net Primary Productivity and Implications for Climate Change, *Annual*
929 *Review of Plant Biology*, 63, 637-661, doi:10.1146/annurev-arplant-042110-103829, 2012.
930 Anav, A., Menut, L., Khvorostyanov, D., and Viovy, N.: Impact of tropospheric ozone on the Euro-
931 Mediterranean vegetation, *Global change biology*, 17, 2342-2359, 2011.
932 Andersen, C. P.: Source-sink balance and carbon allocation below ground in plants exposed to
933 ozone, *New Phytologist*, 157, 213-228, [10.1046/j.1469-8137.2003.00674.x](#), 2003.
934 Arneth, A., Harrison, S. P., Zaehle, S., Tsigaridis, K., Menon, S., Bartlein, P. J., Feichter, J., Korhola, A.,
935 Kulmala, M., O'Donnell, D., Schurgers, G., Sorvari, S., and Vesala, T.: Terrestrial biogeochemical
936 feedbacks in the climate system, *Nature Geosci*, 3, 525-532,
937 http://www.nature.com/ngeo/journal/v3/n8/supinfo/ngeo905_S1.html, 2010.
938 Avnery, S., Mauzerall, D. L., Liu, J., and Horowitz, L. W.: Global crop yield reductions due to surface
939 ozone exposure: 1. Year 2000 crop production losses and economic damage, *Atmospheric*
940 *Environment*, 45, 2284-2296, <https://doi.org/10.1016/j.atmosenv.2010.11.045>, 2011.

Field Code Changed

941 Baig, S., Medlyn, B. E., Mercado, L. M., and Zaehle, S.: Does the growth response of woody plants to
942 elevated CO₂ increase with temperature? A model-oriented meta-analysis, *Global Change Biology*,
943 21, 4303-4319, 10.1111/gcb.12962, 2015.

944 Bellamy, P. H., Loveland, P. J., Bradley, R. I., Lark, R. M., and Kirk, G. J.: Carbon losses from all soils
945 across England and Wales 1978–2003, *Nature*, 437, 245-248, 2005.

946 Bernacchi, C. J., Calfapietra, C., Davey, P. A., Wittig, V. E., Scarascia-Mugnozza, G. E., Raines, C. A.,
947 and Long, S. P.: Photosynthesis and stomatal conductance responses of poplars to free-air CO₂
948 enrichment (PopFACE) during the first growth cycle and immediately following coppice., *New*
949 *Phytologist*, 159, 609-621, 2003.

950 Best, M. J., Pryor, M., Clark, D. B., Rooney, G. G., Essery, R. L. H., Menard, C. B., Edwards, J. M.,
951 Hendry, M. A., Porson, N., Gedney, N., Mercado, L. M., Sitch, S., Blyth, E., Boucher, O., Cox, P. M.,
952 Grimmond, C. S. B., and Harding, R. J.: The Joint UK Land Environment Simulator (JULES), Model
953 description - Part 1: Energy and water fluxes, *Geoscientific Model Development Discussions*, 4, 595-
954 640, 10.5194/GMDD-4-595-2011, 2011.

955 Betts, R. A., Boucher, O., Collins, M., Cox, P. M., Falloon, P. D., Gedney, N., Hemming, D. L.,
956 Huntingford, C., Jones, C. D., and Sexton, D. M.: Projected increase in continental runoff due to plant
957 responses to increasing carbon dioxide, *Nature*, 448, 1037-1041, 2007.

958 Boden, T. A., Marland, G., and Andres, R. J.: Global, Regional, and National Fossil-Fuel CO₂ Emissions,
959 Oak Ridge National Laboratory, U.S. Department of Energy, Oak Ridge, Tenn., USA, 2013.

960 Büker, P., Feng, Z., Uddling, J., Briolat, A., Alonso, R., Braun, S., Elvira, S., Gerosa, G., Karlsson, P. E.,
961 Le Thiec, D., Marzuoli, R., Mills, G., Oksanen, E., Wieser, G., Wilkinson, M., and Emberson, L. D.: New
962 flux based dose-response relationships for ozone for European forest tree species, *Environmental*
963 *Pollution*, 163-174, 2015.

964 Calvete-Sogo, H., Elvira, S., Sanz, J., González-Fernández, I., García-Gómez, H., Sánchez-Martín, L.,
965 Alonso, R., and Bermejo-Bermejo, V.: Current ozone levels threaten gross primary production and
966 yield of Mediterranean annual pastures and nitrogen modulates the response, *Atmospheric*
967 *Environment*, 95, 197-206, <http://dx.doi.org/10.1016/j.atmosenv.2014.05.073>, 2014.

968 Capriel, P.: Trends in organic carbon and nitrogen contents in agricultural soils in Bavaria (south
969 Germany) between 1986 and 2007, *European Journal of Soil Science*, 64, 445-454, 2013.

970 Cech, P. G., Pepin, S., and Korner, C.: Elevated CO₂ reduces sap flux in mature deciduous forest trees,
971 *Oecologia*, 137, 258-268, 2003.

972 Ceulemans, R., and Mousseau, M.: Effects of elevated atmospheric CO₂ on woody plants, *New*
973 *Phytologist*, 127, 1994.

974 Ciais, P., Wattenbach, M., Vuichard, N., Smith, P., Piao, S., Don, A., Luysaert, S., Janssens, I.,
975 Bondeau, A., and Dechow, R.: The European carbon balance. Part 2: croplands, *Global Change*
976 *Biology*, 16, 1409-1428, 2010.

977 Ciais, P., Sabine, C., Bala, G., Bopp, L., Brovkin, V., Canadell, J., Chhabra, A., DeFries, R., Galloway, J.,
978 Heimann, M., Jones, C., Le Quéré, C., Myneni, R. B., Piao, S., and Thornton, P.: Carbon and Other
979 Biogeochemical Cycles. In: *Climate Change 2013: The Physical Science Basis. Contribution of Working*
980 *Group I to the Fifth Assessment Report of the Intergovernmental Panel on Climate Change* [Stocker,
981 T.F., D. Qin, G.-K. Plattner, M. Tignor, S.K. Allen, J. Boschung, A. Nauels, Y. Xia, V. Bex and P.M.
982 Midgley (eds.)]. Cambridge University Press, Cambridge, United Kingdom and New York, NY, USA.,
983 2013.

984 Clark, D. B., Mercado, L. M., Sitch, S., Jones, C. D., Gedney, N., Best, M. J., Pryor, M., Rooney, G. G.,
985 Essery, R. L. H., Blyth, E., Boucher, O., Harding, R. J., and Cox, P. M.: The Joint UK Land Environment
986 Simulator (JULES), Model description - Part 2: Carbon fluxes and vegetation, *Geoscientific Model*
987 *Development Discussions*, 4, 641-688, 10.5194/gmdd-4-641-2011, 2011.

988 CLRTAP: The UNECE Convention on Long-range Transboundary Air Pollution. Manual on
989 Methodologies and Criteria for Modelling and Mapping Critical Loads and Levels and Air Pollution
990 Effects, Risks and Trends: Chapter III Mapping Critical Levels for Vegetation, accessed via,

991 [http://icpvegetation.ceh.ac.uk/publications/documents/Chapter3-](http://icpvegetation.ceh.ac.uk/publications/documents/Chapter3-Mappingcriticallevelsforvegetation_000.pdf)
992 [Mappingcriticallevelsforvegetation_000.pdf](http://icpvegetation.ceh.ac.uk/publications/documents/Chapter3-Mappingcriticallevelsforvegetation_000.pdf), 2017.

993 Collins, W. J., Sitch, S., and Boucher, O.: How vegetation impacts affect climate metrics for ozone
994 precursors, *Journal of Geophysical Research: Atmospheres*, 115, D23308, 10.1029/2010JD014187,
995 2010.

996 Collins, W. J., Bellouin, N., Doutriaux-Boucher, M., Gedney, N., Halloran, P., Hinton, T., Hughes, J.,
997 Jones, C. D., Joshi, M., Liddicoat, S., Martin, G., O'Connor, F., Rae, J., Senior, C., Sitch, S., Totterdell, I.,
998 Wiltshire, A., and Woodward, S.: Development and evaluation of an Earth-System model –
999 HadGEM2, *Geosci. Model Dev.*, 4, 1051-1075, 10.5194/gmd-4-1051-2011, 2011.

1000 Cooper, O. R., Parrish, D. D., Stohl, A., Trainer, M., Nedelec, P., Thouret, V., Cammas, J. P., Oltmans,
1001 S. J., Johnson, B. J., Tarasick, D., Leblanc, T., McDermid, I. S., Jaffe, D., Gao, R., Stith, J., Ryerson, T.,
1002 Aikin, K., Campos, T., Weinheimer, A., and Avery, M. A.: Increasing springtime ozone mixing ratios in
1003 the free troposphere over western North America, *Nature*, 463, 344-348,
1004 http://www.nature.com/nature/journal/v463/n7279/supinfo/nature08708_S1.html, 2010.

1005 Cooper, O. R., Parrish, D., Ziemke, J., Balashov, N., Cupeiro, M., Galbally, I., Gilge, S., Horowitz, L.,
1006 Jensen, N., and Lamarque, J.-F.: Global distribution and trends of tropospheric ozone: An
1007 observation-based review, *Elementa: Science of the Anthropocene*, 2, 000029, 2014.

1008 Cox, P. M., Betts, R. A., Jones, C. D., Spall, S. A., and Totterdell, I. J.: Acceleration of global warming
1009 due to carbon-cycle feedbacks in a coupled climate model, *Nature*, 408, 184-187, 2000.

1010 Cox, P. M.: Description of the TRIFFID dynamic global vegetation model, Hadley Centre technical
1011 note 24, 2001.

1012 Cruz, F. T., Pitman, A. J., and Wang, Y. P.: Can the stomatal response to higher atmospheric carbon
1013 dioxide explain the unusual temperatures during the 2002 Murray-Darling Basin drought?, *Journal of*
1014 *Geophysical Research: Atmospheres*, 115, 2010.

1015 de Arellano, J. V.-G., van Heerwaarden, C. C., and Lelieveld, J.: Modelled suppression of boundary-
1016 layer clouds by plants in a CO₂-rich atmosphere, *Nature geoscience*, 5, 701-704, 2012.

1017 De Kauwe, M., Kala, J., Lin, Y.-S., Pitman, A., Medlyn, B., Duursma, R., Abramowitz, G., Wang, Y.-P.,
1018 and Miralles, D.: A test of an optimal stomatal conductance scheme within the CABLE land surface
1019 model, 8, 431-452, 2015.

1020 Dentener, F., Stevenson, D., Ellingsen, K., van Noije, T., Schultz, M., Amann, M., Atherton, C., Bell, N.,
1021 Bergmann, D., Bey, I., Bouwman, L., Butler, T., Cofala, J., Collins, B., Drevet, J., Doherty, R., Eickhout,
1022 B., Eskes, H., Fiore, A., Gauss, M., Hauglustaine, D., Horowitz, L., Isaksen, I. S. A., Josse, B., Lawrence,
1023 M., Krol, M., Lamarque, J. F., Montanaro, V., Müller, J. F., Peuch, V. H., Pitari, G., Pyle, J., Rast, S.,
1024 Rodriguez, J., Sanderson, M., Savage, N. H., Shindell, D., Strahan, S., Szopa, S., Sudo, K., Van
1025 Dingenen, R., Wild, O., and Zeng, G.: The Global Atmospheric Environment for the Next Generation,
1026 *Environmental Science & Technology*, 40, 3586-3594, 10.1021/es0523845, 2006.

1027 Derwent, R. G., Stevenson, D. S., Doherty, R. M., Collins, W. J., Sanderson, M. G., and Johnson, C. E.:
1028 Radiative forcing from surface NO_x emissions: spatial and seasonal variations, *Climatic Change*, 88,
1029 385-401, 10.1007/s10584-007-9383-8, 2008.

1030 Ellsworth, D. S.: CO₂ enrichment in a maturing pine forest: are CO₂ exchange and water status in the
1031 canopy affected?, *Plant, Cell and Environment*, 22, 461-472, 1999.

1032 Emberson, L. D., Ashmore, M. R., Cambridge, H. M., Simpson, D., and Tuovinen, J.-P.: Modelling
1033 stomatal ozone flux across Europe, *Environmental Pollution*, 109, 403-413, 2000.

1034 Emberson, L. D., Simpson, D., Tuovinen, J.-P., Ashmore, M. R., and Cambridge, H. M.: Modelling and
1035 mapping ozone deposition in Europe, *Water Air Soil Pollution*, 130, 577-582, 2001.

1036 Engardt, M., Simpson, D., Schwikowski, M., and Granat, L.: Deposition of sulphur and nitrogen in
1037 Europe 1900-2050. Model calculations and comparison to historical observations, *Tellus B: Chem.*
1038 *Phys. Meteor.*, 69, 2017.

1039 Etheridge, D. M., Steele, L. P., Langenfelds, R. L., Francey, R. J., M., B., and Morgan, V. I.: Natural and
1040 anthropogenic changes in atmospheric CO₂ over the last 1000 years from air in Antarctic ice and firn,
1041 *Journal of Geophysical Research*, 101(D2), 4115-4128, doi:10.1029/95JD03410, 1996.

1042 Fagnano, M., Maggio, A., and Fumagalli, I.: Crops' responses to ozone in Mediterranean
1043 environments, *Environmental Pollution*, 157, 1438-1444, 2009.

1044 Fares, S., Vargas, R., Detto, M., Goldstein, A. H., Karlik, J., Paoletti, E., and Vitale, M.: Tropospheric
1045 ozone reduces carbon assimilation in trees: estimates from analysis of continuous flux
1046 measurements, *Global change biology*, 19, 2427-2443, 2013.

1047 Felzer, B., Reilly, J., Melillo, J., Kicklighter, D., Sarofim, M., Wang, C., Prinn, R., and Zhuang, Q.: Future
1048 Effects of Ozone on Carbon Sequestration and Climate Change Policy Using a Global Biogeochemical
1049 Model, *Climatic Change*, 73, 345-373, 10.1007/s10584-005-6776-4, 2005.

1050 Felzer, B. S. F., Kicklighter, D. W., Melillo, J. M., Wang, C., Zhuang, Q., and Prinn, R. G.: Ozone effects
1051 on net primary productivity and carbon sequestration in the conterminous United States using a
1052 biogeochemistry model, *Tellus*, 56B, 230-248, 2004.

1053 Feng, Z., Kobayashi, K., and Ainsworth, E. A.: Impact of elevated ozone concentration on growth,
1054 physiology, and yield of wheat (*Triticum aestivum* L.): a meta-analysis, *Global Change Biology*, 14,
1055 2696-2708, 10.1111/j.1365-2486.2008.01673.x, 2008.

1056 Fowler, D., Flechard, C., Cape, J. N., Storeton-West, R. L., and Coyle, M.: Measurements of Ozone
1057 Deposition to Vegetation Quantifying the Flux, the Stomatal and Non-Stomatal Components, *Water,
1058 Air, and Soil Pollution*, 130, 63-74, 10.1023/a:1012243317471, 2001.

1059 Fowler, D., Pilegaard, K., Sutton, M., Ambus, P., Raivonen, M., Duyzer, J., Simpson, D., Fagerli, H.,
1060 Fuzzi, S., and Schjørring, J. K.: Atmospheric composition change: ecosystems-atmosphere
1061 interactions, *Atmospheric Environment*, 43, 5193-5267, 2009.

1062 Franz, M., Simpson, D., Arneth, A., and Zaehle, S.: Development and evaluation of an ozone
1063 deposition scheme for coupling to a terrestrial biosphere model, *Biogeosciences*, 14, 45-71,
1064 doi:10.5194/bg-14-45-2017, 2017.

1065 Friedlingstein, P., Cox, P., Betts, R., Bopp, L., von Bloh, W., Brovkin, V., Cadule, P., Doney, S., Eby, M.,
1066 Fung, I., Bala, G., John, J., Jones, C., Joos, F., Kato, T., Kawamiya, M., Knorr, W., Lindsay, K.,
1067 Matthews, H. D., Raddatz, T., Rayner, P., Reick, C., Roeckner, E., Schnitzler, K. G., Schnur, R.,
1068 Strassmann, K., Weaver, A. J., Yoshikawa, C., and Zeng, N.: Climate-Carbon Cycle Feedback Analysis:
1069 Results from the C4MIP Model Intercomparison, *Journal of Climate*, 19, 3337-3353,
1070 10.1175/jcli3800.1, 2006.

1071 Fuhrer, J., Val Martin, M., Mills, G., Heald, C. L., Harmens, H., Hayes, F., Sharps, K., Bender, J., and
1072 Ashmore, M. R.: Current and future ozone risks to global terrestrial biodiversity and ecosystem
1073 processes, *Ecology and Evolution*, 6, 8785-8799, 10.1002/ece3.2568, 2016.

1074 Gedney, N., Cox, P. M., Bett, R. A., Boucher, O., Huntingford, C., and Stott, P. A.: Detection of a direct
1075 carbon dioxide effect in continental river runoff records, *Nature*, 439, 835-838, 2006.

1076 Grantz, D., Gunn, S., and VU, H. B.: O₃ impacts on plant development: a meta-analysis of root/shoot
1077 allocation and growth, *Plant, cell & environment*, 29, 1193-1209, 2006.

1078 Harmens, H., Mills, G., Emberson, L. D., and Ashmore, M. R.: Implications of climate change for the
1079 stomatal flux of ozone: A case study for winter wheat, *Environmental Pollution*, 146, 763-770,
1080 <http://dx.doi.org/10.1016/j.envpol.2006.05.018>, 2007.

1081 Hayes, F., Wagg, S., Mills, G., Wilkinson, S., and Davies, W.: Ozone effects in a drier climate:
1082 implications for stomatal fluxes of reduced stomatal sensitivity to soil drying in a typical grassland
1083 species, *Global Change Biology*, 18, 948-959, 2012.

1084 Heikkinen, J., Ketoja, E., Nuutinen, V., and Regina, K.: Declining trend of carbon in Finnish cropland
1085 soils in 1974-2009, *Global Change Biology*, 19, 1456-1469, 10.1111/gcb.12137, 2013.

1086 Hofmockel, K. S., Zak, D. R., Moran, K. K., and Jastrow, J. D.: Changes in forest soil organic matter
1087 pools after a decade of elevated CO₂ and O₃, *Soil Biology and Biochemistry*, 43, 1518-1527,
1088 <http://dx.doi.org/10.1016/j.soilbio.2011.03.030>, 2011.

1089 Hoshika, Y., Watanabe, M., Inada, N., and Koike, T.: Ozone-induced stomatal sluggishness develops
1090 progressively in Siebold's beech (*Fagus crenata*), *Environmental Pollution*, 166, 152-156, 2012a.

1091 Hoshika, Y., Omasa, K., and Paoletti, E.: Whole-Tree Water Use Efficiency Is Decreased by Ambient
1092 Ozone and Not Affected by O₃-Induced Stomatal Sluggishness, PLOS ONE, 7, e39270,
1093 10.1371/journal.pone.0039270, 2012b.

1094 Hoshika, Y., Watanabe, M., Inada, N., and Koike, T.: Model-based analysis of avoidance of ozone
1095 stress by stomatal closure in Siebold's beech (*Fagus crenata*), Annals of Botany, 112, 1149-1158,
1096 2013.

1097 Hoshika, Y., Katata, G., Deushi, M., Watanabe, M., Koike, T., and Paoletti, E.: Ozone-induced stomatal
1098 sluggishness changes carbon and water balance of temperate deciduous forests., Scientific Reports,
1099 doi:10.1038/srep09871, 2015.

1100 Hurtt, G., Chini, L. P., Froking, S., Betts, R., Feddema, J., Fischer, G., Fisk, J., Hibbard, K., Houghton,
1101 R., Janetos, A., and Jones, C. D.: Harmonization of land-use scenarios for the period 1500–2100: 600
1102 years of global gridded annual land-use transitions, wood harvest, and resulting secondary lands,
1103 Climatic Change, 109, 117-161, 2011.

1104 IPCC: Climate change 2013: The Physical Science Basis, IPCC Working Group I Contribution to AR5,
1105 2013.

1106 Jacobs, C. M. J.: Direct impact of atmospheric CO₂ enrichment on regional transpiration, Wageningen
1107 Agricultural University, 1994.

1108 Janssens, I. A., Freibauer, A., Ciais, P., Smith, P., Nabuurs, G.-J., Folberth, G., Schlamadinger, B.,
1109 Hutjes, R. W. A., Ceulemans, R., Schulze, E.-D., Valentini, R., and Dolman, A. J.: Europe's Terrestrial
1110 Biosphere Absorbs 7 to 12% of European Anthropogenic CO₂ Emissions, Science, 300, 1538-1542,
1111 10.1126/science.1083592, 2003.

1112 Jones, C. D., Cox, P., and Huntingford, C.: Uncertainty in climate–carbon-cycle projections associated
1113 with the sensitivity of soil respiration to temperature, Tellus B, 55, 642-648, 10.1034/j.1600-
1114 0889.2003.01440.x, 2003.

1115 Jung, M., Reichstein, M., Margolis, H. A., Cescatti, A., Richardson, A. D., Arain, M. A., Arneth, A.,
1116 Bernhofer, C., Bonal, D., Chen, J., Gianelle, D., Gobron, N., Kiely, G., Kutsch, W., Lasslop, G., Law, B.
1117 E., Lindroth, A., Merbold, L., Montagnani, L., Moors, E. J., Papale, D., Sottocornola, M., Vaccari, F.,
1118 and Williams, C.: Global patterns of land-atmosphere fluxes of carbon dioxide, latent heat, and
1119 sensible heat derived from eddy covariance, satellite, and meteorological observations, Journal of
1120 Geophysical Research: Biogeosciences, 116, n/a-n/a, 10.1029/2010JG001566, 2011.

1121 Kala, J., De Kauwe, M. G., Pitman, A. J., Medlyn, B. E., Wang, Y. P., Lorenz, R., and Perkins-Kirkpatrick,
1122 S. E.: Impact of the representation of stomatal conductance on model projections of heatwave
1123 intensity., Scientific Reports, 1-7, 10.1038/srep23418, 2016.

1124 Karlsson, P. E., Braun, S., Broadmeadow, M., Elvira, S., Emberson, L., Gimeno, B. S., Le Thiec, D.,
1125 Novak, K., Oksanen, E., Schaub, M., Uddling, J., and Wilkinson, M.: Risk assessments for forest trees:
1126 The performance of the ozone flux versus the AOT concepts, Environmental Pollution, 146, 608-616,
1127 <http://dx.doi.org/10.1016/j.envpol.2006.06.012>, 2007.

1128 Karnosky, D., Percy, K. E., Xiang, B., Callan, B., Noormets, A., Mankovska, B., Hopkin, A., Sober, J.,
1129 Jones, W., and Dickson, R.: Interacting elevated CO₂ and tropospheric O₃ predisposes aspen
1130 (*Populus tremuloides* Michx.) to infection by rust (*Melampsora medusae* f. sp. *tremuloideae*), Global
1131 Change Biology, 8, 329-338, 2002.

1132 Karnosky, D. F., Skelly, J. M., Percy, K. E., and Chappelka, A. H.: Perspectives regarding 50years of
1133 research on effects of tropospheric ozone air pollution on US forests, Environmental Pollution, 147,
1134 489-506, 2007.

1135 Keeling, C. D., and Whorf, T. P.: Atmospheric CO₂ records from sites in the SIO air sampling network.
1136 In Trends: A Compendium of Data on Global Change, Carbon Dioxide Information Analysis Center,
1137 Oak Ridge National Laboratory, Oak Ridge, Tenn., U.S.A. , 2004.

1138 Kitao, M., Löw, M., Heerd, C., Grams, T. E., Häberle, K.-H., and Matyssek, R.: Effects of chronic
1139 elevated ozone exposure on gas exchange responses of adult beech trees (*Fagus sylvatica*) as related
1140 to the within-canopy light gradient, Environmental Pollution, 157, 537-544, 2009.

1141 Kjellström, E., Nikulin, G., Hansson, U., Strandberg, G., and Ullerstig, A.: 21st century changes in the
1142 European climate: uncertainties derived from an ensemble of regional climate model simulations,
1143 *Tellus A*, 63, 24-40, 2011.

1144 Kubiske, M., Quinn, V., Marquardt, P., and Karnosky, D.: Effects of Elevated Atmospheric CO₂ and/or
1145 O₃ on Intra- and Interspecific Competitive Ability of Aspen, *Plant biology*, 9, 342-355, 2007.

1146 Lamarque, J., Shindell, D. T., Josse, B., Young, P., Cionni, I., Eyring, V., Bergmann, D., Cameron-Smith,
1147 P., Collins, W. J., and Doherty, R.: The Atmospheric Chemistry and Climate Model Intercomparison
1148 Project (ACCMIP): overview and description of models, simulations and climate diagnostics,
1149 *Geoscientific Model Development*, 6, 179-206, 2013.

1150 Langner, J., Engardt, M., Baklanov, A., Christensen, J. H., Gauss, M., Geels, C., Hedegaard, G. B.,
1151 Nuterman, R., Simpson, D., and Soares, J.: A multi-model study of impacts of climate change on
1152 surface ozone in Europe, *Atmospheric Chemistry and Physics*, 12, 10423-10440, 2012a.

1153 Langner, J., Engardt, M., and Andersson, C.: European summer surface ozone 1990–2100,
1154 *Atmospheric Chemistry and Physics*, 12, 10097-10105, 2012b.

1155 Le Quéré, C., Moriarty, R., Andrew, R. M., Peters, G. P., Ciais, P., Friedlingstein, P., Jones, S. D., Sitch,
1156 S., Tans, P., Arneeth, A., Boden, T. A., Bopp, L., Bozec, Y., Canadell, J. G., Chini, L. P., Chevallier, F.,
1157 Cosca, C. E., Harris, I., Hoppema, M., Houghton, R. A., House, J. I., Jain, A. K., Johannessen, T., Kato,
1158 E., Keeling, R. F., Kitidis, V., Klein Goldewijk, K., Koven, C., Landa, C. S., Landschützer, P., Lenton, A.,
1159 Lima, I. D., Marland, G., Mathis, J. T., Metzl, N., Nojiri, Y., Olsen, A., Ono, T., Peng, S., Peters, W., Pfeil,
1160 B., Poulter, B., Raupach, M. R., Regnier, P., Rödenbeck, C., Saito, S., Salisbury, J. E., Schuster, U.,
1161 Schwinger, J., Séférian, R., Segschneider, J., Steinhoff, T., Stocker, B. D., Sutton, A. J., Takahashi, T.,
1162 Tilbrook, B., van der Werf, G. R., Viovy, N., Wang, Y. P., Wanninkhof, R., Wiltshire, A., and Zeng, N.:
1163 Global carbon budget 2014, *Earth Syst. Sci. Data*, 7, 47-85, 10.5194/essd-7-47-2015, 2015.

1164 Le Quéré, C., Andrew, R. M., Canadell, J. G., Sitch, S., Korsbakken, J. I., Peters, G. P., Manning, A. C.,
1165 Boden, T. A., Tans, P. P., Houghton, R. A., Keeling, R. F., Alin, S., Andrews, O. D., Anthoni, P., Barbero,
1166 L., Bopp, L., Chevallier, F., Chini, L. P., Ciais, P., Currie, K., Delire, C., Doney, S. C., Friedlingstein, P.,
1167 Gkritzalis, T., Harris, I., Hauck, J., Haverd, V., Hoppema, M., Klein Goldewijk, K., Jain, A. K., Kato, E.,
1168 Körtzinger, A., Landschützer, P., Lefèvre, N., Lenton, A., Lienert, S., Lombardozi, D., Melton, J. R.,
1169 Metzl, N., Millero, F., Monteiro, P. M. S., Munro, D. R., Nabel, J. E. M. S., Nakaoka, S. I., O'Brien, K.,
1170 Olsen, A., Omar, A. M., Ono, T., Pierrot, D., Poulter, B., Rödenbeck, C., Salisbury, J., Schuster, U.,
1171 Schwinger, J., Séférian, R., Skjelvan, I., Stocker, B. D., Sutton, A. J., Takahashi, T., Tian, H., Tilbrook, B.,
1172 van der Laan-Luijckx, I. T., van der Werf, G. R., Viovy, N., Walker, A. P., Wiltshire, A. J., and Zaehle, S.:
1173 Global Carbon Budget 2016, *Earth Syst. Sci. Data*, 8, 605-649, 10.5194/essd-8-605-2016, 2016.

1174 Le Quéré, C., Andrew, R. M., Friedlingstein, P., Sitch, S., Pongratz, J., Manning, A. C., Korsbakken, J. I.,
1175 Peters, G. P., Canadell, J. G., Jackson, R. B., Boden, T. A., Tans, P. P., Andrews, O. D., Arora, V. K.,
1176 Bakker, D. C. E., Barbero, L., Becker, M., Betts, R. A., Bopp, L., Chevallier, F., Chini, L. P., Ciais, P.,
1177 Cosca, C. E., Cross, J., Currie, K., Gasser, T., Harris, I., Hauck, J., Haverd, V., Houghton, R. A., Hunt, C.
1178 W., Hurtt, G., Ilyina, T., Jain, A. K., Kato, E., Kautz, M., Keeling, R. F., Klein Goldewijk, K., Körtzinger,
1179 A., Landschützer, P., Lefèvre, N., Lenton, A., Lienert, S., Lima, I., Lombardozi, D., Metzl, N., Millero,
1180 F., Monteiro, P. M. S., Munro, D. R., Nabel, J. E. M. S., Nakaoka, S.-I., Nojiri, Y., Padín, X. A., Pregon,
1181 A., Pfeil, B., Pierrot, D., Poulter, B., Rehder, G., Reimer, J., Rödenbeck, C., Schwinger, J., Séférian, R.,
1182 Skjelvan, I., Stocker, B. D., Tian, H., Tilbrook, B., van der Laan-Luijckx, I. T., van der Werf, G. R., van
1183 Heuven, S., Viovy, N., Vuichard, N., Walker, A. P., Watson, A. J., Wiltshire, A. J., Zaehle, S., and Zhu,
1184 D.: Global Carbon Budget 2017, *Earth Syst. Sci. Data Discuss*, in review, 2017.

1185 Leuzinger, S., and Körner, C.: Water savings in mature deciduous forest trees under elevated CO₂,
1186 *Global Change Biology*, 13, 2498-2508, doi:10.1111/j.1365-2486.2007.01467.x, 2007.

1187 Lin, Y.-S., Medlyn, B. E., Duursma, R. A., Prentice, I. C., Wang, H., Baig, S., Eamus, D., de Dios, V. R.,
1188 Mitchell, P., and Ellsworth, D. S.: Optimal stomatal behaviour around the world, *Nature Climate
1189 Change*, 5, 459-464, 2015.

1190 Lindroth, R. L.: Impacts of Elevated Atmospheric CO₂ and O₃ on Forests: Phytochemistry, Trophic
1191 Interactions, and Ecosystem Dynamics, *Journal of Chemical Ecology*, 36, 2-21, 10.1007/s10886-009-
1192 9731-4, 2010.

1193 Logan, J. A., Staehelin, J., Megretskaia, I. A., Cammas, J. P., Thouret, V., Claude, H., De Backer, H.,
1194 Steinbacher, M., Scheel, H. E., Stübi, R., Fröhlich, M., and Derwent, R.: Changes in ozone over
1195 Europe: Analysis of ozone measurements from sondes, regular aircraft (MOZAIC) and alpine surface
1196 sites, *Journal of Geophysical Research*, 117, 1-23, 2012.

1197 Lombardozi, D., Levis, S., Bonan, G., Hess, P. G., and Sparks, J. P.: The Influence of Chronic Ozone
1198 Exposure on Global Carbon and Water Cycles, *Journal of Climate*, 28, 292-305, 10.1175/jcli-d-14-
1199 00223.1, 2015.

1200 Long, S. P., Ainsworth, E. A., Leakey, A. D. B., Nosberger, J., and Ort, D. R.: Food for Thought: Lower-
1201 Than-Expected Crop Yield Stimulation with Rising CO₂ Concentrations, *Science*, 312, 1918-1921,
1202 10.1126/science.1114722, 2006.

1203 Löw, M., Herbinger, K., Nunn, A., Häberle, K.-H., Leuchner, M., Heerd, C., Werner, H., Wipfler, P.,
1204 Pretzsch, H., and Tausz, M.: Extraordinary drought of 2003 overrules ozone impact on adult beech
1205 trees (*Fagus sylvatica*), *Trees*, 20, 539-548, 2006.

1206 Loya, W. M., Pregitzer, K. S., Karberg, N. J., King, J. S., and Giardina, C. P.: Reduction of soil carbon
1207 formation by tropospheric ozone under increased carbon dioxide levels., *Nature*, 425, 705-707,
1208 2003.

1209 Luysaert, S., Abril, G., Andres, R., Bastviken, D., Bellassen, V., Bergamaschi, P., Bousquet, P.,
1210 Chevallier, F., Ciais, P., Corazza, M., Dechow, R., Erb, K. H., Etiope, G., Fortems-Cheiney, A., Grassi, G.,
1211 Hartmann, J., Jung, M., Lathière, J., Lohila, A., Mayorga, E., Moosdorf, N., Njakou, D. S., Otto, J.,
1212 Papale, D., Peters, W., Peylin, P., Raymond, P., Rödenbeck, C., Saarnio, S., Schulze, E. D., Szopa, S.,
1213 Thompson, R., Verkerk, P. J., Vuichard, N., Wang, R., Wattenbach, M., and Zaehle, S.: The European
1214 land and inland water CO₂, CO, CH₄ and N₂O balance between 2001 and 2005, *Biogeosciences*, 9,
1215 3357-3380, 10.5194/bg-9-3357-2012, 2012.

1216 Massman, W. J.: A review of the molecular diffusivities of H₂O, CO₂, CH₄, CO, O₃, SO₂, NH₃, N₂O,
1217 NO, and NO₂ in air, O₂ and N₂ near STP, *Atmospheric Environment*, 32, 1111-1127,
1218 [http://dx.doi.org/10.1016/S1352-2310\(97\)00391-9](http://dx.doi.org/10.1016/S1352-2310(97)00391-9), 1998.

1219 Matyssek, R., Wieser, G., Ceulemans, R., Rennenberg, H., Pretzsch, H., Haberer, K., Löw, M., Nunn,
1220 A., Werner, H., and Wipfler, P.: Enhanced ozone strongly reduces carbon sink strength of adult beech
1221 (*Fagus sylvatica*)—Resume from the free-air fumigation study at Kranzberg Forest, *Environmental*
1222 *Pollution*, 158, 2527-2532, 2010a.

1223 Matyssek, R., Karnosky, D., Wieser, G., Percy, K., Oksanen, E., Grams, T., Kubiske, M., Hanke, D., and
1224 Pretzsch, H.: Advances in understanding ozone impact on forest trees: messages from novel
1225 phytotron and free-air fumigation studies, *Environmental Pollution*, 158, 1990-2006, 2010b.

1226 McLaughlin, S. B., Nosal, M., Wullschleger, S. D., and Sun, G.: Interactive effects of ozone and climate
1227 on tree growth and water use in a southern Appalachian forest in the USA, *New Phytologist*, 174,
1228 109-124, 10.1111/j.1469-8137.2007.02018.x, 2007a.

1229 McLaughlin, S. B., Wullschleger, S. D., Sun, G., and Nosal, M.: Interactive effects of ozone and climate
1230 on water use, soil moisture content and streamflow in a southern Appalachian forest in the USA,
1231 *New Phytologist*, 174, 125-136, 10.1111/j.1469-8137.2007.01970.x, 2007b.

1232 Medlyn, B. E., Badeck, F. W., De Pury, D. G. G., Barton, C. V. M., Broadmeadow, M., Ceulemans, R.,
1233 De Angelis, P., Forstreuter, M., Jach, M. E., Kellomaki, S., Laitat, E., Marek, M., Philippot, S., Rey, A.,
1234 Strassmeyer, J., Laitinen, K., Liozon, R., Portier, B., Roberntz, P., Wang, K., and Jstbid, P. G.: Effects
1235 of elevated [CO₂] on photosynthesis in European forest species: a meta-analysis of model
1236 parameters, *Plant, Cell & Environment*, 22, 1475-1495, doi:10.1046/j.1365-3040.1999.00523.x, 1999.

1237 Medlyn, B. E., Barton, C. V. M., Broadmeadow, M. S. J., Ceulemans, R., De Angelis, P., Forstreuter,
1238 M., Freeman, M., Jackson, S. B., Kellomaki, S., Laitat, E., Rey, A., Roberntz, P., Sigurdsson, B. D.,
1239 Strassmeyer, J., Wang, K., Curtis, P. S., and Jarvis, P. G.: Stomatal conductance of forest species

1240 after long-term exposure to elevated CO₂ concentration: a synthesis, *New Phytologist*, 149, 247-264,
1241 2001.

1242 Medlyn, B. E., Duursma, R. A., Eamus, D., Ellsworth, D. S., Prentice, I. C., Barton, C. V., Crous, K. Y., de
1243 Angelis, P., Freeman, M., and Wingate, L.: Reconciling the optimal and empirical approaches to
1244 modelling stomatal conductance, *Global Change Biology*, 17, 2134-2144, 2011.

1245 Mercado, L. M., Bellouin, N., Sitch, S., Boucher, O., Huntingford, C., Wild, M., and Cox, P. M.: Impact
1246 of changes in diffuse radiation on the global land carbon sink, *Nature*, 458, 1014-1017,
1247 http://www.nature.com/nature/journal/v458/n7241/supinfo/nature07949_S1.html, 2009.

1248 Mills, G., Hayes, F., Wilkinson, S., and Davies, W. J.: Chronic exposure to increasing background
1249 ozone impairs stomatal functioning in grassland species, *Global Change Biology*, 15, 1522-1533,
1250 2009.

1251 Mills, G., Hayes, F., Simpson, D., Emberson, L., Norris, D., Harmens, H., and BÜKer, P.: Evidence of
1252 widespread effects of ozone on crops and (semi-)natural vegetation in Europe (1990–2006) in
1253 relation to AOT40- and flux-based risk maps, *Global Change Biology*, 17, 592-613, 10.1111/j.1365-
1254 2486.2010.02217.x, 2011b.

1255 Mills, G., Harmens, H., Wagg, S., Sharps, K., Hayes, F., Fowler, D., Sutton, M., and Davies, B.: Ozone
1256 impacts on vegetation in a nitrogen enriched and changing climate, *Environmental Pollution*, 208,
1257 898-908, 2016.

1258 Norby, R. J., Wullschlegel, S. D., Gunderson, C. A., Johnson, D. W., and Ceulemans, R.: Tree responses
1259 to rising CO₂ in field experiments: implications for the future forest, *Plant, Cell and Environment*, 22,
1260 683-714, 1999.

1261 Norby, R. J., DeLucia, E. H., Gielen, B., Calfapietra, C., Giardina, C. P., King, J. S., Ledford, J., McCarthy,
1262 H. R., Moore, D. J. P., Ceulemans, R., De Angelis, P., Finzi, A. C., Karnosky, D. F., Kubiske, M. E., Lukac,
1263 M., Pregitzer, K. S., Scarascia-Mugnozza, G. E., Schlesinger, W. H., and Oren, R.: Forest response to
1264 elevated CO₂ is conserved across a broad range of productivity, *Proc. Natl. Acad. Sci. U. S. A.*, 102,
1265 18052-18056, 10.1073/pnas.0509478102, 2005.

1266 Nunn, A. J., Reiter, I. M., Häberle, K.-H., Langebartels, C., Bahnweg, G., Pretzsch, H., Sandermann, H.,
1267 and Matyssek, R.: Response patterns in adult forest trees to chronic ozone stress: identification of
1268 variations and consistencies, *Environmental Pollution*, 136, 365-369, 2005.

1269 Pacifico, F., Folberth, G. A., Jones, C. D., Harrison, S. P., and Collins, W. J.: Sensitivity of biogenic
1270 isoprene emissions to past, present, and future environmental conditions and implications for
1271 atmospheric chemistry, *Journal of Geophysical Research: Atmospheres*, 117, n/a-n/a,
1272 10.1029/2012JD018276, 2012.

1273 Paoletti, E., and Grulke, N. E.: Ozone exposure and stomatal sluggishness in different plant
1274 physiognomic classes, *Environmental Pollution*, 158, 2664-2671, 2010.

1275 Parrish, D. D., Law, K. S., Staehelin, J., Derwent, R., Cooper, O. R., Tanimoto, H., Volz-Thomas, A.,
1276 Gilge, S., Scheel, H. E., Steinbacher, M., and Chan, E.: Long-term changes in lower tropospheric
1277 baseline ozone concentrations at northern mid-latitudes, *Atmos. Chem. Phys.*, 12, 11485-11504,
1278 10.5194/acp-12-11485-2012, 2012.

1279 Percy, K. E., Awmack, C. S., Lindroth, R. L., Kubiske, M. E., Kopper, B. J., Isebrands, J., Pregitzer, K. S.,
1280 Hendrey, G. R., Dickson, R. E., and Zak, D. R.: Altered performance of forest pests under atmospheres
1281 enriched by CO₂ and O₃, *Nature*, 420, 403-407, 2002.

1282 Royal-Society: Ground-level ozone in the 21st century: future trends, impacts and policy
1283 implications, *Science Policy Report 15/08*, 2008.

1284 Samuelsson, P., Jones, C. G., Willén, U., Ullerstig, A., Gollvik, S., Hansson, U., Jansson, C., Kjellström,
1285 E., Nikulin, G., and Wyser, K.: The Rossby Centre Regional Climate model RCA3: model description
1286 and performance, *Tellus A*, 63, 4-23, 2011.

1287 Saxe, H., Ellsworth, D. S., and Heath, J.: Tree and forest functioning in an enriched CO₂ atmosphere,
1288 *New Phytologist*, 139, 395-436, doi:10.1046/j.1469-8137.1998.00221.x, 1998.

1289 Schulze, E.-D., Ciais, P., Luyssaert, S., Schrumppf, M., Janssens, I. A., Thiruchittampalam, B., Theloke, J.,
1290 Saurat, M., Bringezu, S., and Lelieveld, J.: The European carbon balance. Part 4: integration of carbon
1291 and other trace-gas fluxes, *Global Change Biology*, 16, 1451-1469, 2010.
1292 Schulze, E. D., Luyssaert, S., Ciais, P., Freibauer, A., Janssens, I. A., and et al.: Importance of methane
1293 and nitrous oxide for Europe's terrestrial greenhouse-gas balance, *Nature Geosci*, 2, 842-850,
1294 http://www.nature.com/ngeo/journal/v2/n12/supinfo/ngeo686_S1.html, 2009.
1295 Sicard, P., De Marco, A., Troussier, F., Renoua, C., Vas, N., and Paoletti, E.: Decrease in surface ozone
1296 concentrations at Mediterranean remote sites and increase in the cities, *Atmospheric Environment*,
1297 79, 705-715, 2013.
1298 Simpson, D., Benedictow, A., Berge, H., Bergström, R., Emberson, L. D., Fagerli, H., Flechard, C. R.,
1299 Hayman, G. D., Gauss, M., and Jonson, J. E.: The EMEP MSC-W chemical transport model—technical
1300 description, *Atmospheric Chemistry and Physics*, 12, 7825-7865, 2012.
1301 Simpson, D., Andersson, C., Christensen, J. H., Engardt, M., Geels, C., Nyiri, A., Posch, M., Soares, J.,
1302 Sofiev, M., and Wind, P.: Impacts of climate and emission changes on nitrogen deposition in Europe:
1303 a multi-model study, *Atmospheric Chemistry and Physics*, 14, 6995-7017, 2014a.
1304 Simpson, D., Arneth, A., Mills, G., Solberg, S., and Uddling, J.: Ozone—the persistent menace:
1305 interactions with the N cycle and climate change, *Current Opinion in Environmental Sustainability*, 9,
1306 9-19, 2014b.
1307 Sitch, S., Cox, P. M., Collins, W. J., and Huntingford, C.: Indirect radiative forcing of climate change
1308 through ozone effects on the land-carbon sink, *Nature*, 448, 791-794,
1309 http://www.nature.com/nature/journal/v448/n7155/supinfo/nature06059_S1.html, 2007.
1310 Sitch, S., Friedlingstein, P., Gruber, N., Jones, S. D., Murray-Tortarolo, G., Ahlström, A., Doney, S. C.,
1311 Graven, H., Heinze, C., Huntingford, C., Levis, S., Levy, P. E., Lomas, M., Poulter, B., Viovy, N., Zaehle,
1312 S., Zeng, N., Arneth, A., Bonan, G., Bopp, L., Canadell, J. G., Chevallier, F., Ciais, P., Ellis, R., Gloor, M.,
1313 Peylin, P., Piao, S. L., Le Quéré, C., Smith, B., Zhu, Z., and Myneni, R.: Recent trends and drivers of
1314 regional sources and sinks of carbon dioxide, *Biogeosciences*, 12, 653-679, 10.5194/bg-12-653-2015,
1315 2015.
1316 Sleutel, S., De Neve, S., and Hofman, G.: Estimates of carbon stock changes in Belgian cropland., *Soil*
1317 *Use and Management*, 19, 166-171, 10.1079/SUM2003187, 2003.
1318 Sun, G. E., McLaughlin, S. B., Porter, J. H., Uddling, J., Mulholland, P. J., Adams, M. B., and Pederson,
1319 N.: Interactive influences of ozone and climate on streamflow of forested watersheds, *Global Change*
1320 *Biology*, 18, 3395-3409, 10.1111/j.1365-2486.2012.02787.x, 2012.
1321 Tai, P. K. A., Val Martin, M., and Heald, C. L.: Threat to future global food security from climate
1322 change and ozone air pollution, *Nature Climate Change*, 4, 817 - 821, 2014.
1323 Talhelm, A. F., Pregitzer, K. S., Kubiske, M. E., Zak, D. R., Company, C. E., Burton, A. J., Dickson, R. E.,
1324 Hendrey, G. R., Isebrands, J. G., Lewin, K. F., Nagy, J., and Karnosky, D. F.: Elevated carbon dioxide
1325 and ozone alter productivity and ecosystem carbon content in northern temperate forests, *Global*
1326 *Change Biology*, 20, 2492-2504, 10.1111/gcb.12564, 2014.
1327 Tricker, P. J., Pecchiari, M., Bunn, S. M., Vaccari, F. P., Peressotti, A., Miglietta, F., and Taylor, G.:
1328 Water use of a bioenergy plantation increases in a future high CO₂ world, *Biomass and Bioenergy*,
1329 33, 200-208, 2009.
1330 Tuovinen, J.-P., Emberson, L., and Simpson, D.: Modelling ozone fluxes to forests for risk assessment:
1331 status and prospects, *Annals of Forest Science*, 66, 1-14, 2009.
1332 Tuovinen, J., Hakola, H., Karlsson, P., and Simpson, D.: Air pollution risks to Northern European
1333 forests in a changing climate, *Climate Change, Air Pollution and Global Challenges Understanding*
1334 *and Perspectives from Forest Research*, 2013.
1335 Uddling, J., Teclaw, R. M., Pregitzer, K. S., and Ellsworth, D. S.: Leaf and canopy conductance in aspen
1336 and aspen-birch forests under free-air enrichment of carbon dioxide and ozone, *Tree Physiology*, 29,
1337 1367-1380, 2009.

1338 Verstraeten, W. W., Neu, J. L., Williams, J. E., Bowman, K. W., Worden, J. R., and Boersma, K. F.:
1339 Rapid increases in tropospheric ozone production and export from China, *Nature Geoscience* 8, 690-
1340 695, 2015.

1341 Vingarzan, R.: A review of surface ozone background levels and trends, *Atmospheric Environment*,
1342 38, 3431-3442, <https://doi.org/10.1016/j.atmosenv.2004.03.030>, 2004.

1343 Weedon, G. P., Gomes, S., Viterbo, P., Österle, H., Adam, J. C., Bellouin, N., Boucher, O., and Best, M.
1344 J.: The WATCH Forcing Data 1958-2001: a meteorological forcing dataset for land surface- and
1345 hydrological models. , *WATCH Tech. Rep.* 22, 41p (available at www.eu-watch.org/publications).
1346 2010.

1347 Weedon, G. P., Gomes, S., Viterbo, P., Shuttleworth, W. J., Blyth, E., Österle, H., Adam, J. C., Bellouin,
1348 N., Boucher, O., and Best, M.: Creation of the WATCH Forcing data and its use to assess global and
1349 regional reference crop evaporation over land during the twentieth century, *Journal of*
1350 *Hydrometeorology*, 12, 823-848, doi: 10.1175/2011JHM1369.1., 2011.

1351 Wilkinson, S., and Davies, W. J.: Ozone suppresses soil drying-and abscisic acid (ABA)-induced
1352 stomatal closure via an ethylene-dependent mechanism, *Plant, Cell & Environment*, 32, 949-959,
1353 2009.

1354 Wilkinson, S., and Davies, W. J.: Drought, ozone, ABA and ethylene: new insights from cell to plant to
1355 community, *Plant, Cell & Environment*, 33, 510-525, 10.1111/j.1365-3040.2009.02052.x, 2010.

1356 Wittig, V. E., Ainsworth, E. A., and Long, S. P.: To what extent do current and projected increases in
1357 surface ozone affect photosynthesis and stomatal conductance of trees? A meta-analytic review of
1358 the last 3 decades of experiments, *Plant, Cell & Environment*, 30, 1150-1162, 10.1111/j.1365-
1359 3040.2007.01717.x, 2007.

1360 Wittig, V. E., Ainsworth, E. A., Naidu, S. L., Karnosky, D. F., and Long, S. P.: Quantifying the impact of
1361 current and future tropospheric ozone on tree biomass, growth, physiology and biochemistry: a
1362 quantitative meta-analysis, *Global Change Biology*, 15, 396-424, 10.1111/j.1365-2486.2008.01774.x,
1363 2009.

1364 Wullschleger, S. D., Gunderson, C. A., Hanson, P. J., Wilson, K. B., and Norby, R. J.: Sensitivity of
1365 stomatal and canopy conductance to elevated CO₂ concentration; interacting variables and
1366 perspectives of scale, *New Phytologist*, 153, 485-496, doi:10.1046/j.0028-646X.2001.00333.x, 2002.

1367 Young, P., Arneth, A., Schurgers, G., Zeng, G., and Pyle, J. A.: The CO₂ inhibition of terrestrial isoprene
1368 emission significantly affects future ozone projections, *Atmospheric Chemistry and Physics*, 9, 2793-
1369 2803, 2009.

1370 Young, P., Archibald, A., Bowman, K., Lamarque, J.-F., Naik, V., Stevenson, D., Tilmes, S., Voulgarakis,
1371 A., Wild, O., and Bergmann, D.: Pre-industrial to end 21st century projections of tropospheric ozone
1372 from the Atmospheric Chemistry and Climate Model Intercomparison Project (ACCMIP),
1373 *Atmospheric Chemistry and Physics*, 13, 2063-2090, 2013.

1374 Zaehle, S.: Terrestrial nitrogen-carbon cycle interactions at the global scale, *Philosophical*
1375 *Transactions of the Royal Society B: Biological Sciences*, 368, 20130125, 10.1098/rstb.2013.0125,
1376 2013.

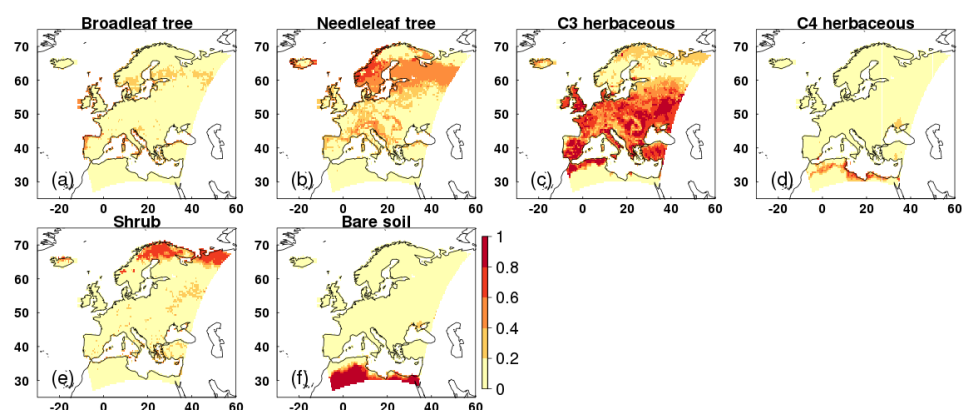
1377 Zak, D. R., Pregitzer, K. S., Kubiske, M. E., and Burton, A. J.: Forest productivity under elevated CO₂
1378 and O₃: positive feedbacks to soil N cycling sustain decade-long net primary productivity
1379 enhancement by CO₂, *Ecology Letters*, 14, 1220-1226, 10.1111/j.1461-0248.2011.01692.x, 2011.

1380
1381
1382
1383
1384
1385
1386

1387 **Supplementary Information**

1388

1389 **S1 Fractional cover of JULES PFTs**



1390

1391 **Figure S1.** Fractional cover of each JULES PFT and bare soil at $0.5^\circ \times 0.5^\circ$ resolution.

1392

1393

1394 **S2 Calibration of O₃ uptake model for European vegetation**

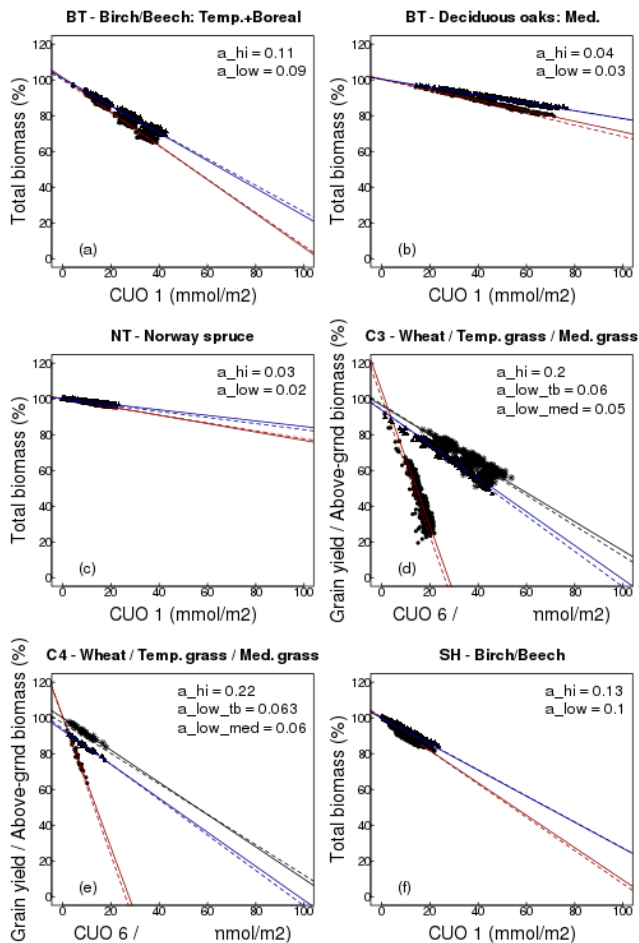
1395

1396 Here we use the latest literature on O₃ dose-response relationships derived from observed field data across Europe
1397 (CLRTAP, 2017) to calculate the key PFT-specific parameters. Data comes from the UNECE CLRTAP (2017)
1398 report which is a synthesis of the latest peer reviewed literature, collated by a panel of experts and so is considered
1399 the state-of the art knowledge. Each PFT was calibrated for a high and low plant O₃ sensitivity to account for
1400 uncertainty in the sensitivity of different plant species to O₃, using the approach of Sitch *et al.*, (2007). In addition,
1401 where possible owing to available data, a distinction was made for Mediterranean regions. This was because the
1402 work of B ker *et al.* (2015) showed that different O₃ dose-response relationships are needed to describe the O₃
1403 sensitivity of dominant Mediterranean trees. For the C₃ herbaceous PFT – the dominant land cover type across
1404 the European domain in this study (Fig. S1) - the O₃ sensitivity was calibrated against observations for wheat to
1405 give a representation of agricultural regions (high plant O₃ sensitivity), versus natural grassland (low plant O₃
1406 sensitivity), with a separate function for Mediterranean grasslands (low plant O₃ sensitivity), all taken from
1407 CLRTAP (2017). Tree/shrub PFTs were calibrated against observed O₃ dose-response functions for the high plant
1408 O₃ sensitivity (BT = Birch/Beech, BT-Med = deciduous oaks, NT = Norway spruce, shrub = Birch/Beech) all

1409 from CLRTAP (2017). The low plant O₃ sensitivity functions for trees/shrubs were calibrated as being 20 % less
1410 sensitive based on the difference in sensitivity between high and low sensitive tree species in the Karlsson et al.
1411 (2007) study. Due to limitations in data availability, the shrub parameterisation uses the observed dose-response
1412 functions for broadleaf trees. Similarly, the parameterisation for C₄ herbaceous uses the observed dose-responses
1413 for C₃ herbaceous, however the fractional cover of C₄ herbs across Europe is low (Fig. S1), so this assumption
1414 affects a very small percentage of land cover. See Table S1 and Figure S2.
1415

1416 To calibrate the O₃ uptake model for the fast carbon fluxes, e.g. net primary productivity (NPP), JULES was run
1417 across Europe forced using the WFDEI observational climate dataset (Weedon, 2013) at 0.5° X 0.5° spatial and
1418 three hour temporal resolution. JULES uses interpolation to disaggregate the forcing data down from 3 hours to
1419 an hourly model time step. The model was spun-up over the period 1979 to 1999 with a fixed atmospheric CO₂
1420 concentration of 368.33 ppm (1999 value from Mauna Loa observations, (Tans and Keeling)). Zero tropospheric
1421 ozone concentration was assumed for the control simulation, for the simulations with O₃, spin-up used spatially
1422 explicit fields of present day O₃ concentration produced using the UK Chemistry and Aerosol (UKCA) model
1423 with standard chemistry from the run evaluated by O'Connor et al. (2014). A fixed land cover map was used based
1424 on IGBP (International Geosphere-Biosphere Programme) land cover classes (IGBP-DIS), therefore as the
1425 vegetation distribution was fixed and the calibration was not looking at carbon stores, a short spin-up was adequate
1426 to equilibrate soil temperature and soil moisture. JULES was then run for year 2000 with a corresponding CO₂
1427 concentration of 369.52 ppm (from Mauna Loa observations, (Tans and Keeling)) and monthly fields of spatially
1428 explicit tropospheric O₃ (O'Connor et al., 2014) as necessary.
1429

1430 Calibration was performed using four simulations: with i) zero tropospheric O₃ concentration, this was the control
1431 simulation (NPP_control), ii) tropospheric O₃ at current ambient concentration (NPP_O3), iii) ambient +20 ppb
1432 (NPP_O3+20) and iv) ambient +40 ppb (NPP_O3+40). The different O₃ simulations (i.e. ambient, ambient + 20
1433 and ambient + 40 ppb) were used to capture the range of O₃ conditions used in constructing the observed O₃ dose-
1434 response relationships deployed for calibration, often these had been constructed under artificially manipulated
1435 conditions of ambient + 40 ppb O₃ for example. For each simulation with O₃, JULES used the observed PFT-
1436 specific threshold value of O₃ uptake (i.e. parameter F_{O_3crit}), and an initial estimate of the parameter 'a' (equation
1437 2). For each PFT and each simulation, hourly estimates of NPP and O₃ uptake for the top sunlit leaf in excess of
1438 F_{O_3crit} were accumulated over a PFT dependent accumulation (i.e. ~6 months for broadleaf trees and shrubs, all
1439 year for needle leaf trees, and ~3 months for herbaceous species, through the growing season). Change in total
1440 NPP over the accumulation period (NPP_O3/+20/+40 divided by NPP_control) was calculated for each O₃
1441 simulation and plotted against the cumulative uptake of O₃ over the same period. The linear regression of this
1442 relationship was calculated, and slope and intercept compared against the observed dose-response relationships.
1443 Values of the parameter 'a' were adjusted, and the procedure repeated until the linear regression through the
1444 simulation points matched that of the observations (Fig. S2). JULES is run to be as comparable as possible to the
1445 dose-based O₃ risk indicator used in CLRTAP (2017), as only the O₃ flux to top of canopy sunlit leaves is
1446 accumulated (i.e. the O₃ flux per projected leaf area). See Table S1 Figure S2.



1447
 1448 **Figure S2.** Calibration of JULES for O₃ impacts on plant productivity for each JULES PFT ; a) broadleaf tree –
 1449 temperate/boreal, b) broadleaf tree Mediterranean, c) Needle leaf tree, d) C₃ herbaceous (split into
 1450 temperate/boreal and Mediterranean for the natural grasslands), e) C₄ herbaceous (split into temperate/boreal and
 1451 Mediterranean for the natural grasslands), and f) shrub. High (red) and low (blue) plant O₃ sensitivities are shown.
 1452 For the herbaceous PFTs the low sensitivity calibration is separate for Mediterranean regions (black). The solid
 1453 line is the regression line through the modelled points, the dashed line is the regression line from the observed
 1454 dose-response relationship. [The x axis is cumulative uptake of O₃ above the critical O₃ threshold (F_{O3crit}).

Commented [ORJ43]: RC1 8)

1455
 1456
 1457

1458
1459
1460

	High Sensitivity				
	BT	NT	C3	C4	SH
F_{O3crit} (nmol/m ² /s)	1.00	1.00	1.00	1.00	1.00
a (mmol/m ²)	0.110	0.030	0.200	0.220	0.130
Function	Birch/Beech: $y=100.2-0.93x$	Norway spruce: $y=99.8-0.22x$	Wheat: $y=100.3-3.85x$	Wheat: $y=100.3-3.85x$	Birch/Beech: $y=100.2-0.93x$
dq_{crit} (kg kg ⁻¹)	0.09	0.06	0.1	0.075	0.1
f_0	0.875	0.875	0.9	0.8	0.9
g_1 (kPa ^{0.5})	3.22	2.22	5.56	1.1	2.24
	Low Sensitivity				
	BT	NT	C3	C4	SH
F_{O3crit} (nmol/m ² /s)	1.00	1.00	1.00	1.00	1.00
a (mmol/m ²)	0.090	0.020	0.060	0.063	0.100
Function	Birch/Beech: $y=100.2-0.74x$	Norway spruce: $y=99.8-0.17x$	Temperate perennial grassland: $y=93.9-0.99x$	Temperate perennial grassland: $y=93.9-0.99x$	Birch/Beech: $y=100.2-0.74x$
	High Sensitivity				
	BT - Med.				
F_{O3crit} (nmol/m ² /s)	1.00				
a (mmol/m ²)	0.040				
Function	Dec. Oaks: $y=100.3-0.32x$				
	Low Sensitivity				
	BT - Med.	C3 - Med.	C4 - Med.		
F_{O3crit} (nmol/m ² /s)	1.00	1.00	1.00		
a (mmol/m ²)	0.030	0.050	0.060		
Function	Dec. Oaks: $y=100.3-0.22x$	Mediterranean annual pasture: $y=97.1-0.85x$	Mediterranean annual pasture: $y=97.1-0.85x$		

1461
1462 **Table S1.** PFT-specific parameter values used in the O₃ uptake and g_s formulation in JULES. F_{O3crit} is the critical
1463 O₃ threshold above which damage occurs, a determines the reduction in photosynthesis with O₃ exposure,
1464 ‘function’ shows the regression equation for the observed functions (x is F_{O3crit}), dq_{crit} (kg kg⁻¹) is a PFT specific

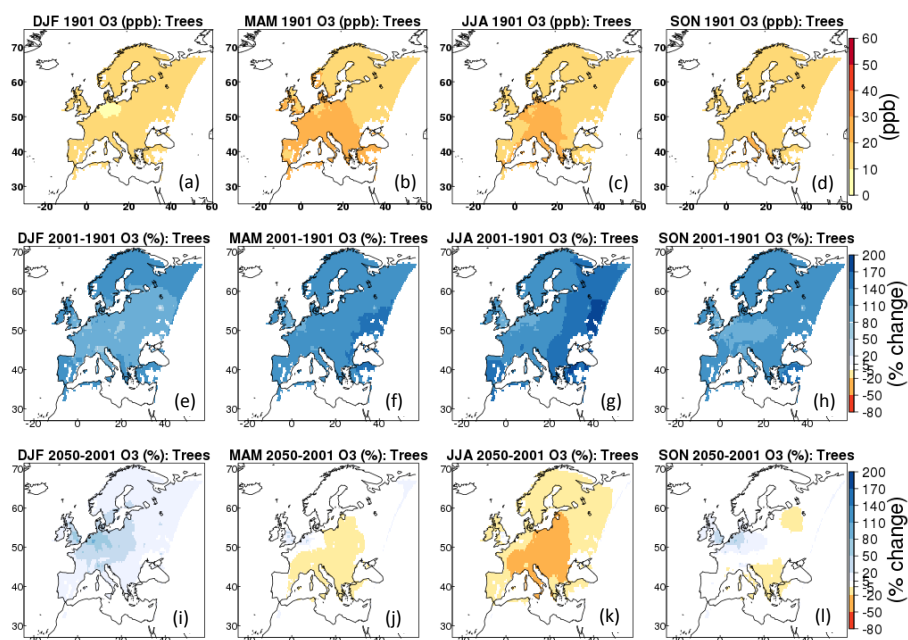
1465 parameters representing the critical humidity deficit at the leaf surface (used in the default JULES g_s model), f_0 is
 1466 the leaf internal to atmospheric CO₂ ratio (c_i/c_a) at the leaf specific humidity deficit (also used in the default
 1467 JULES g_s model), and g_l is the PFT specific parameter of the Medlyn *et al.*, (2011) g_s model. The parameters
 1468 dq_{crit} , f_0 and g_l vary by PFT, but not by O₃ sensitivity so are only shown once here.

1469

1470

1471

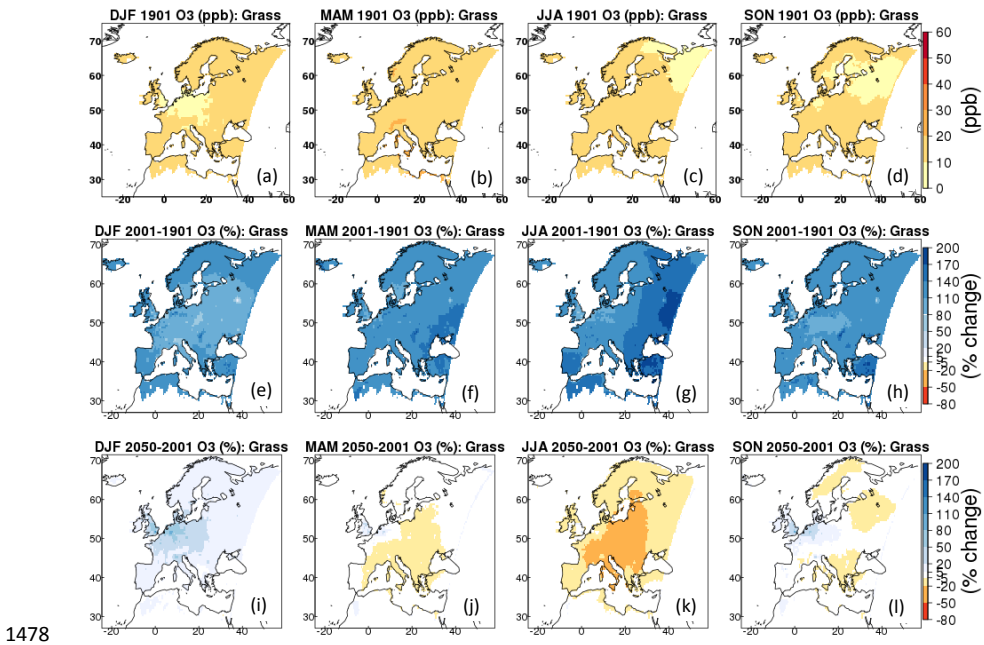
1472



1473

1474 **Figure S3.** (a-d) 1901 seasonal mean (DJF, MAM, JJA, SON) O₃ concentration (ppb) from EMEP for woody
 1475 (tree and shrub) PFTs; (e-h) change in seasonal O₃ concentration (%) from 1901 to 2001; (i-l) change in seasonal
 1476 O₃ concentration (%) from 2001 to 2050.

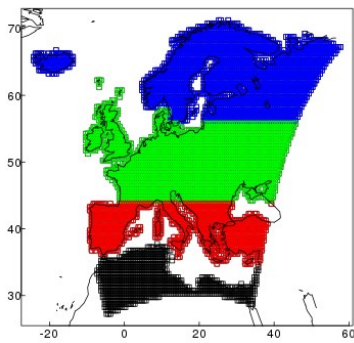
1477



1478

1479 **Figure S4.** (a-d) 1901 seasonal mean (DJF, MAM, JJA, SON) O₃ concentration (ppb) from EMEP for herbaceous
 1480 PFTs; (e-h) change in seasonal O₃ concentration (%) from 1901 to 2001; (i-l) change in seasonal O₃ concentration
 1481 (%) from 2001 to 2050.

1482



1483

1484 **Figure S5.** Regions, blue is Boreal, green is Temperate, red is Mediterranean.

1485

1486

1487 **S3 Assessing the difference between g_s model formulation**

1488

1489 Here we assess the impact of g_s model formulation, comparing the standard JULES Jacobs (1994) formulation
1490 (equation 6; JAC) with the alternative Medlyn *et al.*, (2011) formulation (equation 7; MED). This was done for
1491 two contrasting grid points (wet/dry) in central Europe with a fixed fractional cover of 20% for each PFT.

1492

1493 JULES was spun-up for 20 years (1979-1999) at two grid points in central Europe representing a wet (lat: 48.25;
1494 lon:, 5.25) and a dry site (lat: 38.25; lon:, -7.75). The modelled soil moisture stress factor (fsmc) at the wet site
1495 ranged from 0.8 to 1.0 over the year 2000 (1.0 indicates no soil moisture stress), and at the dry site fsmc steadily
1496 declined from 0.8 at the start of the year to 0.25 by the end of the summer. The WFDEI meteorological forcing
1497 dataset was used (Weedon, 2013), along with atmospheric CO₂ concentration for the year 1999 (368.33 ppm), and
1498 either no O₃ (i.e. the O₃ damage model was switched off) for the control simulations, or spatially explicit fields of
1499 present day O₃ concentration produced using the UK Chemistry and Aerosol (UKCA) model from the run
1500 evaluated by O'Connor *et al.* (2014) for the simulations with O₃. Following the spin-up period, JULES was run
1501 for one year (2000) with corresponding atmospheric CO₂ concentration, and tropospheric O₃ concentrations as
1502 described above. The control and ozone simulations were performed for both JAC and MED model formulations.
1503 Land cover for the spin-up and main run was fixed at 20% for each PFT. For the simulations including O₃ damage,
1504 the high plant O₃ sensitivity parameterisation was used. The difference between these simulations was used to
1505 assess the impact of g_s model formulation on the leaf level fluxes of carbon and water.

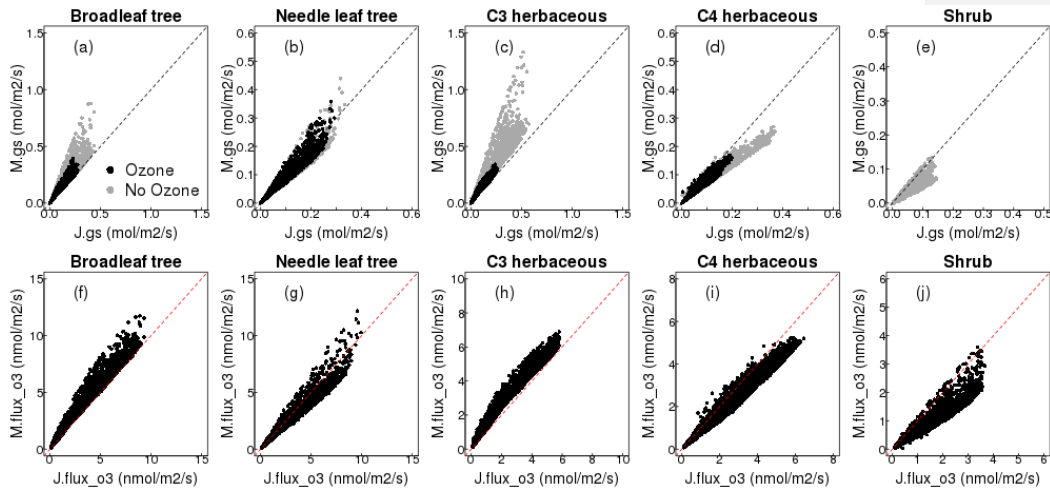
1506

1507 We calculate and report in the main manuscript (results section 3.1), the difference in mean annual leaf-level
1508 water-use that results from the above simulation using the different g_s models. For each day of the simulation we
1509 calculate the percentage difference in water-use between the two simulations, we then calculate the mean and
1510 standard deviation over the year to give the annual mean leaf-level water-use.

1511

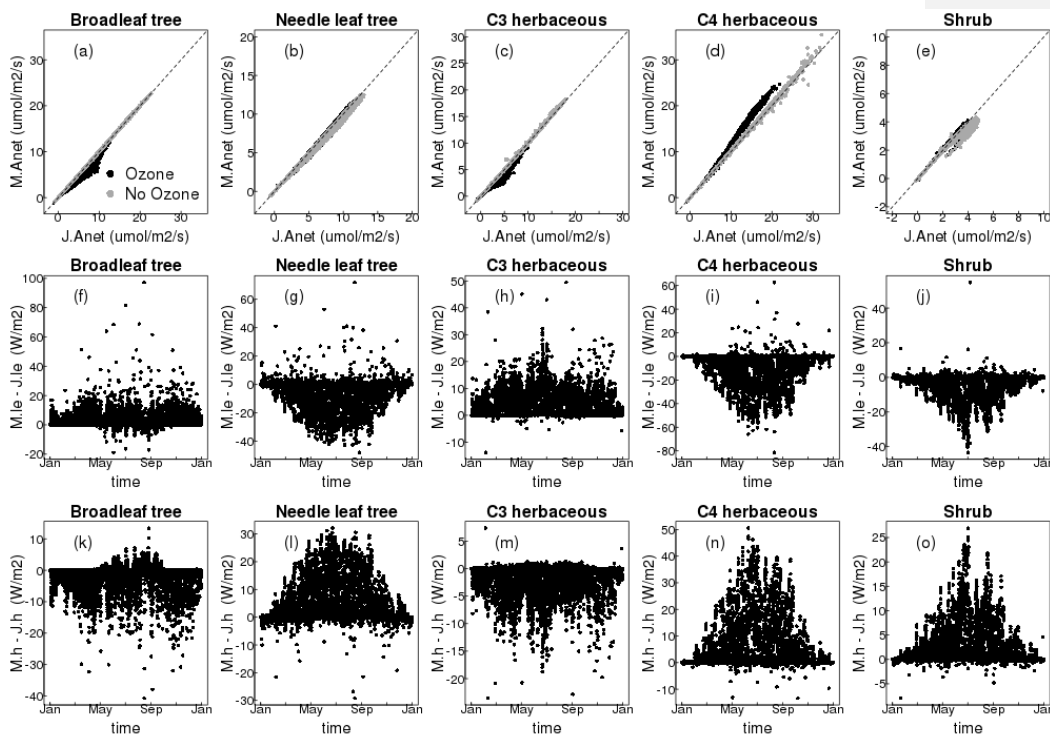
Commented [ORJ44]: RC1 10)

1512

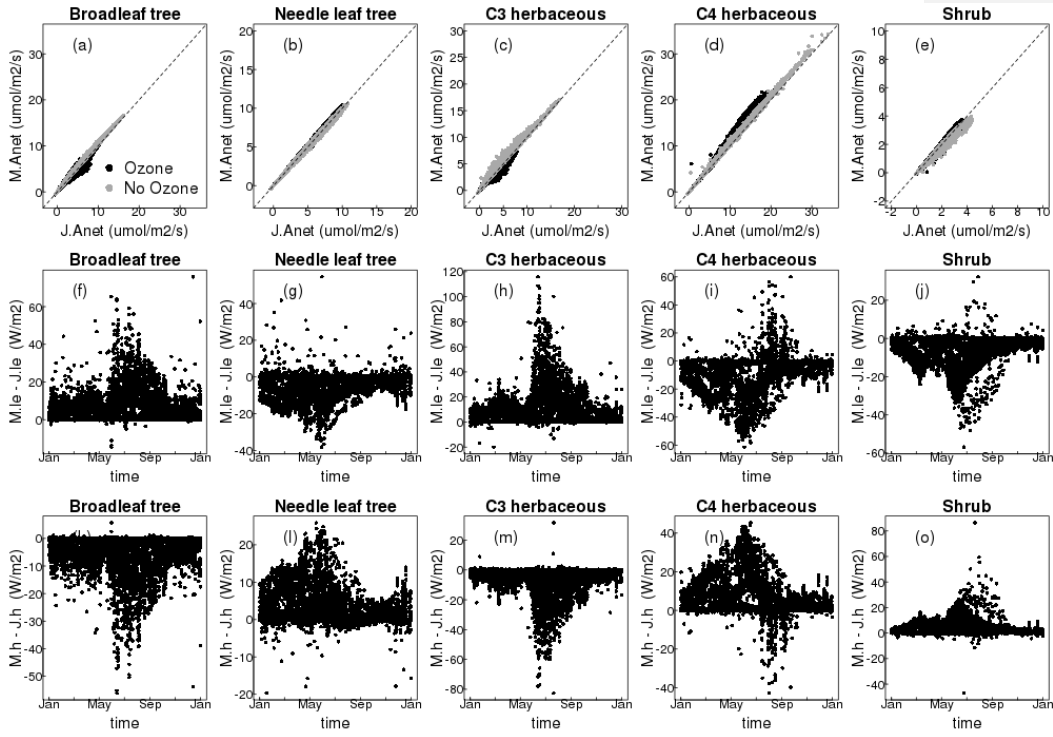


1513 **Figure S6.** Comparison of the Medlyn *et al.*, (2011) g_s model (y axis) versus the Jacobs (1994) g_s model (x axis)
 1514 currently used in JULES for all five JULES PFTs, for stomatal conductance (g_s , top row) and the flux of O_3
 1515 through the stomata ($flux_{o3}$, bottom row) for a dry site.

1516



1517 **Figure S7.** Comparison of the Medlyn *et al.*, (2011) g_s model (y axis) versus the Jacobs (1994) g_s model (x axis)
 1518 currently used in JULES for all five JULES PFTs at a wet site, for net photosynthesis (*Anet*, top row). Residual
 1519 plots (Medlyn - Jacobs) show the difference between models over the year for latent heat (le, middle row) and
 1520 sensible heat (h, bottom row).



1521
 1522 **Figure S8.** Comparison of the Medlyn *et al.*, (2011) g_s model (y axis) versus the Jacobs (1994) g_s model (x axis)
 1523 currently used in JULES for all five JULES PFTs at a dry site, for net photosynthesis (*Anet*, top row). Residual
 1524 plots (Medlyn - Jacobs) show the difference between models over the year for latent heat (le, middle row) and
 1525 sensible heat (h, bottom row).

1526

1527 **S4 Site level evaluation of g_s models**

1528 We carried out site-level simulations using sites from the FLUXNET2015 dataset to evaluate the seasonal cycle
 1529 of latent and sensible heat using the two g_s models JAC and MED compared to observations. Sites were selected
 1530 to represent a range of land cover types (Table S2). In general, at all sites the MED model improved the seasonal
 1531 cycle of both fluxes (lower RMSE), but the magnitude of this varied from site to site. At the deciduous broadleaf
 1532 site US-UMB, MED resulted in large improvements of the simulated seasonal cycle particularly in the summer
 1533 months for both fluxes. At the second deciduous broadleaf site IT-CA1 however, there was almost no difference

1534 between the two g_s models. Both evergreen needleleaf forest sites (FI-Hyy and DE-Tha) saw large improvements
 1535 in the simulated seasonal cycles of latent and sensible heat with the MED model, primarily as a result of lower
 1536 latent heat flux in the spring and summer months, and higher sensible heat flux over the same period. With the
 1537 MED model the monthly mean latent heat flux was improved at the C₃ grass site (CH-Cha) as a result of increased
 1538 flux in the summer months, however there was no improvement in the sensible heat flux and RMSE with MED
 1539 was increased. At the C₄ grass site (US-SRG), small improvements were made in the seasonal cycle of both latent
 1540 and sensible heat with the MED model. At the deciduous savannah site (CG-Tch) which included a high
 1541 proportion of shrub PFT in the land cover type used in the site simulation, large improvements in the seasonal
 1542 cycle of both fluxes were simulated with the MED model, as a result of a decrease in the latent heat flux and an
 1543 increase in the sensible heat flux.

1544

Site name	Country	Latitude	Longitude	Simulated years	Land cover	Dominant PFT(s)
US-UMB	USA	45.56	-84.71	2000-2014	Broadleaf forest	100% BT
IT-CA1	Italy	42.38	12.02	2011-2014	Broadleaf forest	100% BT
FI-Hyy	Finland	62	24.3	1996-2014	Needleleaf forest	100% NT
DE-Tha	Germany	51	13.57	1996-2014	Needleleaf forest	100% NT
CH_Ch	Switzerland	47.21	8.41	2006-2014	C ₃ grassland	80% C ₃ , 20% bare soil
US-SRG	USA	31.8	-110.83	2008-2014	C ₄ grassland	80% C ₄ , 20% bare soil 50% BT, 15% C ₄ , 25% shrub, 10% bare soil
CG-Tch	Congo	-4.5	11.66	2006-2009	Deciduous savanna	soil

1545 **Table S2.** Sites from the FLUXNET2015 dataset used in the site simulations to evaluate g_s models.

1546

1547

1548

1549

1550

1551

1552

1553

1554

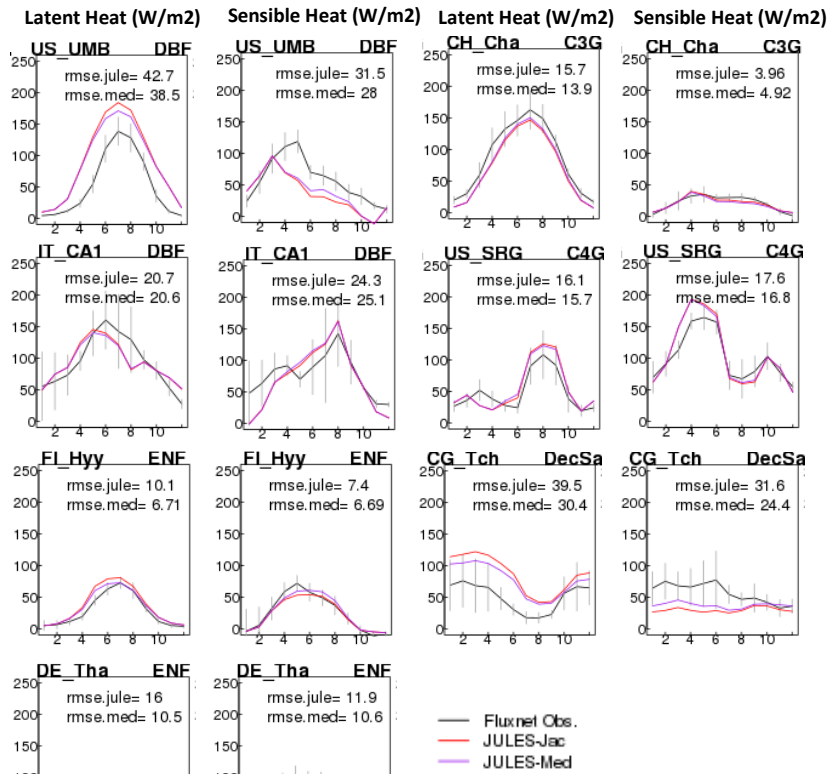
1555

1556

1557

1558

1559
1560
1561
1562
1563
1564
1565
1566
1567
1568
1569
1570
1571
1572
1573
1574
1575

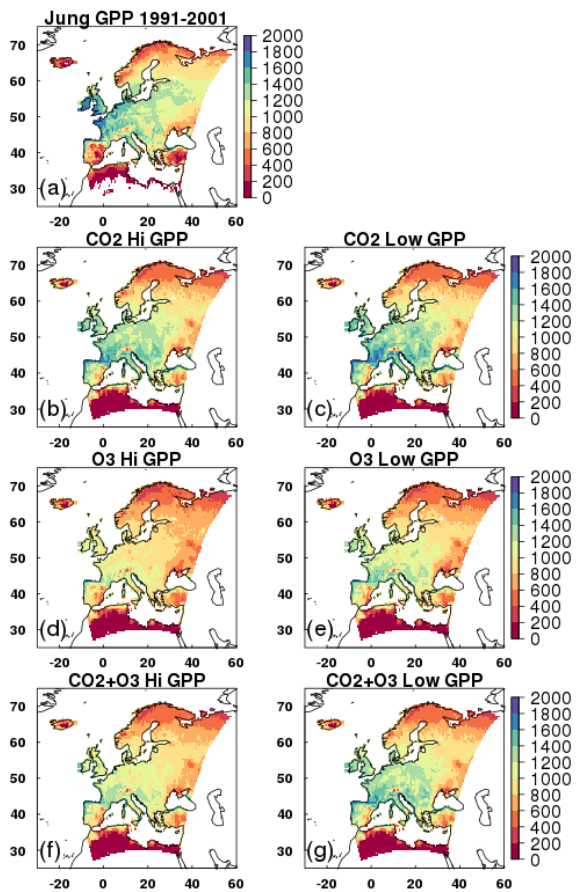


1576 **Fig. S9** Monthly mean fluxes of latent and sensible heat. Observations \pm standard deviation from
1577 FLUXNET2015 sites are shown as black line with grey vertical bars, JULES with the JAC g_s model is shown in
1578 red and JULES with the MED g_s model are shown in purple. Also shown are the root mean squared error (rmse)
1579 for each simulation.

1580
1581
1582

S5 Evaluation of JULES O₃ model

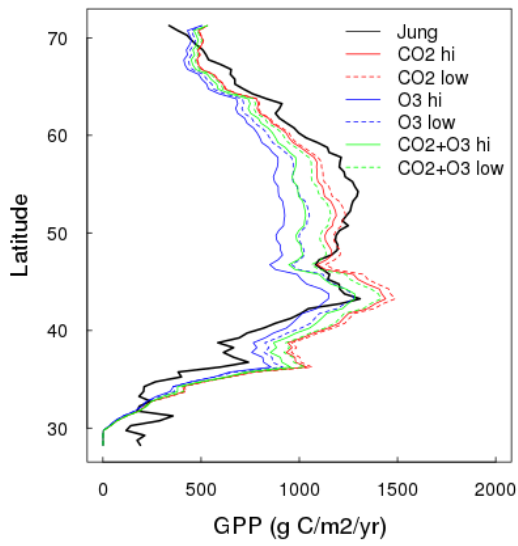
Commented [ORJ45]: RC2 3)
Site level evaluation of the g_s formulations.



1583

1584 **Figure S10.** Mean GPP ($\text{g C m}^{-2} \text{yr}^{-1}$) from 1991 to 2001 for a) the observations based globally extrapolated Flux
 1585 Network model tree ensemble (MTE) (Jung et al., 2011); b, c) model simulations with transient CO_2 and fixed
 1586 O_3 ; d, e) model simulations with fixed CO_2 and transient O_3 , and f, g) our model simulations with transient CO_2
 1587 and transient O_3 . All model simulations show GPP for high and low plant O_3 sensitivity respectively.

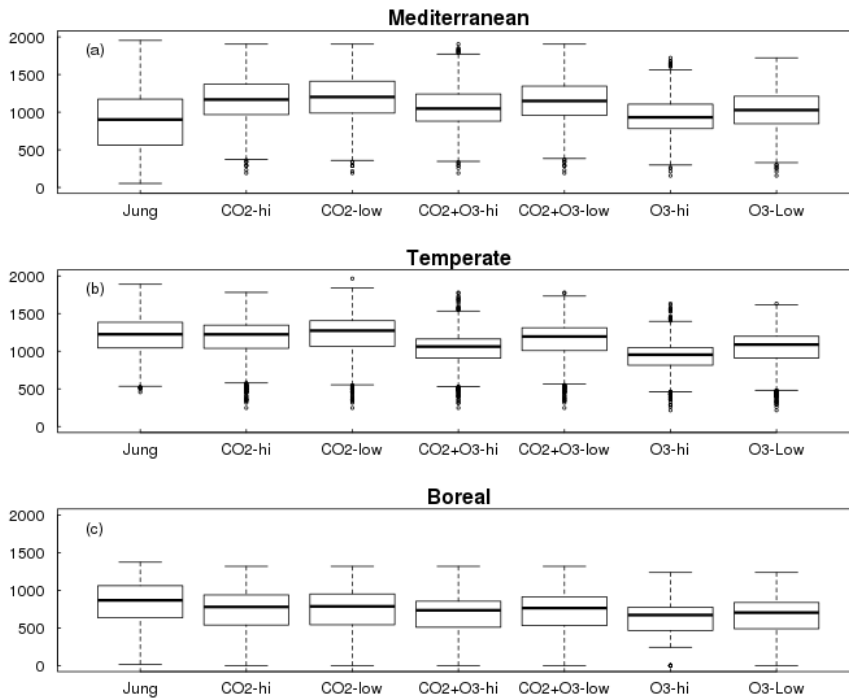
1588



1589

1590 **Figure S11.** Zonal mean GPP from 1991 to 2001 for FLUXNET-MTE (Jung) and all JULES scenario
 1591 simulations with both high (solid lines) and low (dashed lines) plant O₃ sensitivity.

1592



1593

1594 **Figure S12.** Mean GPP from 1991 to 2001 shown by region, comparing MTE (Jung) and all JULES scenario
 1595 simulations with both high and low plant O₃ sensitivity.

Commented [ORJ46]: RC2 3)

1596

1597 **S6 Estimation of effects due to O₃, CO₂ and O₃ with CO₂**

1598

1599 For each variable analysed (GPP, NPP, vegetation carbon, soil carbon, total land carbon and *g_s*), we use the mean
 1600 over 10 years to represent each time period, e.g. the mean over 2040 to 2050 is what we call 2050, 1901 to 1910
 1601 is what we refer to as 1901. The difference between the simulations gives the effect of O₃ and CO₂ either separately
 1602 or in combination over the different time periods. We look at the percentage change due to either O₃ at pre-
 1603 industrial CO₂ concentration (i.e. without the additional effect of atmospheric CO₂ on stomatal behaviour), CO₂
 1604 (at fixed pre-industrial O₃ concentration) or the combined effect of both gases, which is calculated as:

1605

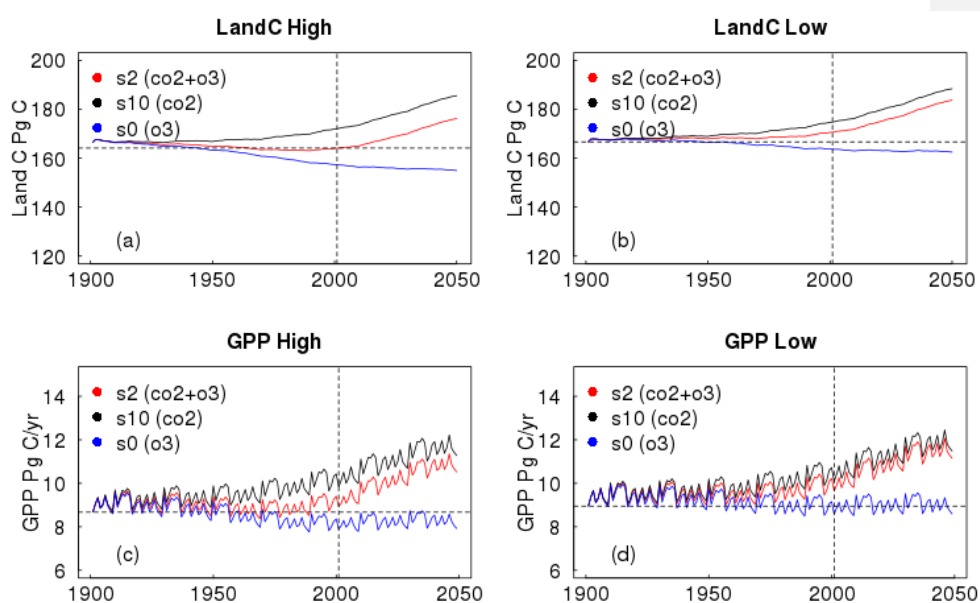
$$1606 \quad 100 * (\text{var}[y_1] - \text{var}[y_2]) / \text{var}[y_2]$$

(S1)

1607

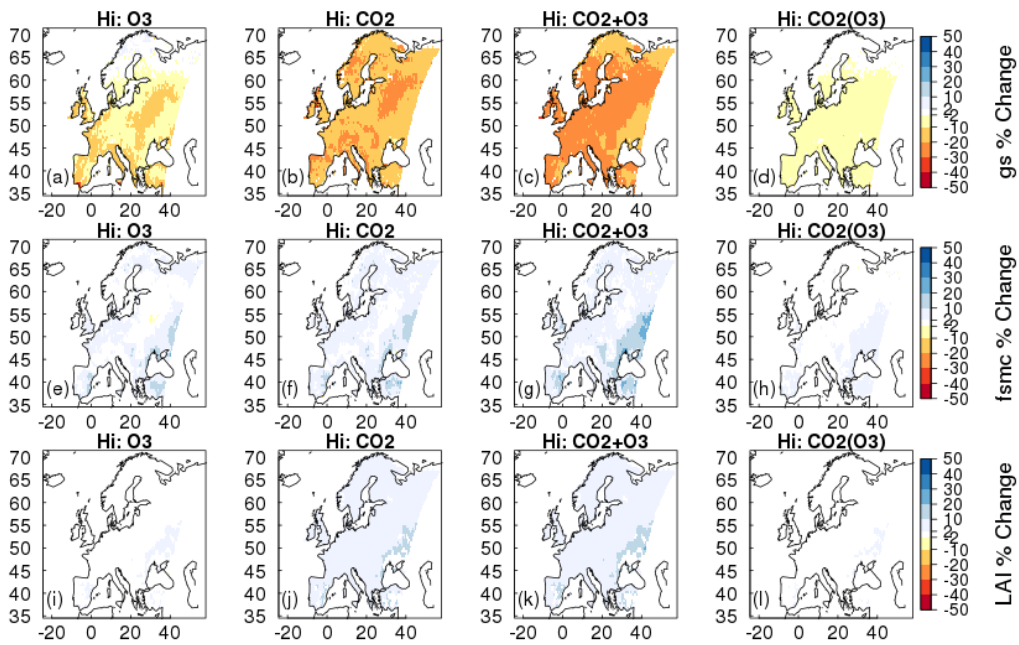
1608
 1609 Where var[*y_x*] represents the variable in time period *y*, e.g. $100 * (\text{varO}_3[2050] - \text{varO}_3[1901]) / \text{varO}_3[1901]$
 1610 gives the O₃ effect (at fixed CO₂) over the full experimental period. The meteorological forcing is prescribed in

1611 these simulations and is therefore the same between the model runs. Other climate factors, such as VPD,
 1612 temperature and soil moisture availability are accounted for in our simulations, but our analysis isolates the effects
 1613 of O₃, CO₂ and O₃ + CO₂.
 1614
 1615
 1616



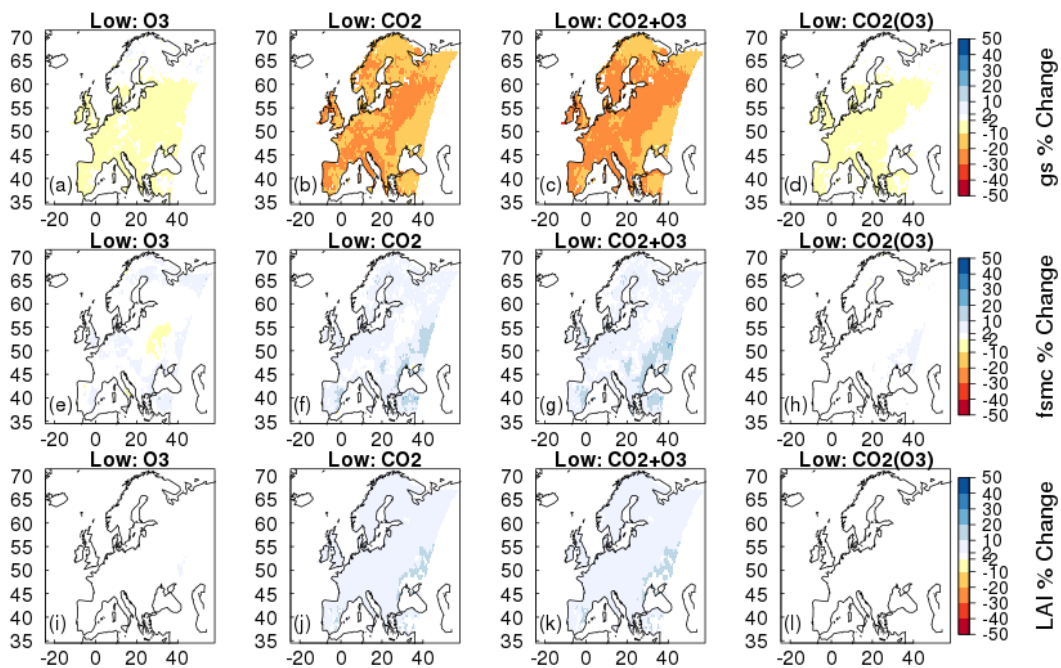
1617
 1618 **Figure S13.** Times series (1901 to 2050) of changes in total carbon stocks (Land C) and gross primary productivity
 1619 (GPP) due to O₃ effects at fixed pre-industrial atmospheric CO₂ concentration (O₃, blue), CO₂ effects at fixed pre-
 1620 industrial O₃ concentration (CO₂, black), and effects of CO₂ and O₃ together (CO₂+O₃, red), for the higher and
 1621 lower plant O₃ sensitivity. The horizontal dashed line shows the pre-industrial value, and the vertical dashed line
 1622 marks the year 2001.

1623
 1624
 1625



1626

1627 **Figure S14.** Simulated percentage change in stomatal conductance (gs) a-c), soil moisture availability factor
 1628 (fsmc) d-e) and leaf area index (LAI) g-i) due to O₃ effects at fixed pre-industrial atmospheric CO₂ concentration
 1629 (O₃), CO₂ effects at fixed pre-industrial O₃ concentration (CO₂), and effects of CO₂ and O₃ changing
 1630 simultaneously (CO₂+O₃). Changes are shown for the periods 1901 to 2050 for the higher plant O₃ sensitivity.
 1631



1632

1633 **Figure S15.** Simulated percentage change in stomatal conductance (gs) a-c), soil moisture availability factor
 1634 (fsmc) d-e) and leaf area index (LAI) g-i) due to O₃ effects at fixed pre-industrial atmospheric CO₂ concentration
 1635 (O₃), CO₂ effects at fixed pre-industrial O₃ concentration (CO₂), and effects of CO₂ and O₃ changing
 1636 simultaneously (CO₂+O₃). Changes are shown for the periods 1901 to 2050 for the lower plant O₃ sensitivity.
 1637

1638

1639

1640

1641

1642

1643

1644

1645

1646

1647

1648
1649
1650
1651
1652

Future run, constant climate (1901 - 2001)						
Hi Sensitivity						
	GPP (Pg C yr ⁻¹)	NPP (Pg C yr ⁻¹)	<i>g_s</i> (m/s)	Veg C (Pg C)	Soil C (Pg C)	Land C (Pg C)
Value in 1901:	9.05	4.46	0.03228	41.1	125.8	167
Absolute diff. (2001 - 1901):						
O₃	-0.81	-0.47	0.00	-0.02	-9.09	-9.21
CO₂	1.16	0.76	0.00	2.82	1.52	4.24
CO₂ + O₃	0.13	0.12	0.00	2.37	-5.55	-3.28
Relative diff. (%)	(%)	(%)	(%)	(%)	(%)	(%)
O₃	-8.95	-10.54	-8.55	-0.05	-7.23	-5.51
CO₂	12.82	17.04	-6.07	6.86	1.21	2.54
CO₂ + O₃	1.44	2.69	-13.66	5.77	-4.41	-1.96
Lower Sensitivity						
	GPP (Pg C yr ⁻¹)	NPP (Pg C yr ⁻¹)	<i>g_s</i> (m/s)	Veg C (Pg C)	Soil C (Pg C)	Land C (Pg C)
Value in 1901:	9.34	4.65	0.03319	41.1	126.4	167.5
Absolute diff. (2001 - 1901):						
O₃	-0.30	-0.21	0.00	-0.21	-3.38	-3.59
CO₂	1.15	0.74	0.00	2.73	3.70	6.43
CO₂ + O₃	0.65	0.43	0.00	2.21	0.29	2.50
Relative diff. (%)	(%)	(%)	(%)	(%)	(%)	(%)
O₃	-3.21	-4.52	-3.31	-0.51	-2.67	-2.14
CO₂	12.31	15.91	-6.39	6.64	2.93	3.84
CO₂ + O₃	6.96	9.25	-9.88	5.38	0.23	1.49

1653
1654
1655
1656
1657
1658
1659

Table S3. Simulated changes in the European land carbon cycle due to changing O₃ and CO₂ concentrations. Shown are changes in total carbon stocks (Land C), split into vegetation (Veg C) and soil (Soil C) carbon, and gross primary productivity (GPP), net primary productivity (NPP) and conductance (*g_s*), between 1901 and 2001.

1660

1661

Future run, constant climate (2001 - 2050)						
Hi Sensitivity						
	GPP (Pg C yr ⁻¹)	NPP (Pg C yr ⁻¹)	g_s (m/s)	Veg C (Pg C)	Soil C (Pg C)	Land C (Pg C)
Value in 2001:						
O₃	8.24	3.99	0.02952	41.08	116.71	157.79
CO₂	10.21	5.22	0.03032	43.92	127.32	171.24
CO₂ + O₃	9.18	4.58	0.02787	43.47	120.25	163.72
Absolute diff. (2050 - 2001):						
O₃	0.01	0.00	0.00	-0.09	-2.35	-2.44
CO₂	1.42	0.95	0.00	5.25	7.73	12.98
CO₂ + O₃	1.66	1.07	0.00	5.11	6.00	11.11
Relative diff. (%)	(%)	(%)	(%)	(%)	(%)	(%)
O₃	0.12	0.00	0.00	-0.22	-2.01	-1.55
CO₂	13.91	18.20	-13.89	11.95	6.07	7.58
CO₂ + O₃	18.08	23.36	-11.37	11.76	4.99	6.79
Lower Sensitivity						
	GPP (Pg C yr ⁻¹)	NPP (Pg C yr ⁻¹)	g_s (m/s)	Veg C (Pg C)	Soil C (Pg C)	Land C (Pg C)
Value in 2001:						
O₃	9.04	4.44	0.03	40.89	123.02	163.91
CO₂	10.49	5.39	0.03	43.83	130.1	173.93
CO₂ + O₃	9.99	5.08	0.02991	43.31	126.69	170
Absolute diff. (2050 - 2001):						
O₃	0.02	-0.06	0.00	-0.13	-0.94	-1.07
CO₂	1.35	0.92	0.00	5.25	7.89	13.14
CO₂ + O₃	1.50	1.00	0.00	5.11	7.25	12.35
Relative diff. (%)	(%)	(%)	(%)	(%)	(%)	(%)
O₃	0.22	-1.35	-0.72	-0.32	-0.76	-0.65
CO₂	12.87	17.07	-14.64	11.98	6.06	7.55
CO₂ + O₃	15.02	19.69	-13.37	11.80	5.72	7.26

1662

1663 **Table S4.** Simulated changes in the European land carbon cycle due to changing O₃ and CO₂ concentrations.

1664 Shown are changes in total carbon stocks (Land C), split into vegetation (Veg C) and soil (Soil C) carbon, and

1665 gross primary productivity (GPP), net primary productivity (NPP) and conductance (g_s), between 2001 and 2050.

1666

1667

1668

1669

Future run, constant climate (1901 - 2050)						
Hi Sensitivity						
	GPP (Pg C yr ⁻¹)	NPP (Pg C yr ⁻¹)	g_s (m/s)	Veg C (Pg C)	Soil C (Pg C)	Land C (Pg C)
Value in 1901:	9.05	4.46	0.03228	41.1	125.8	167
Absolute diff. (2050 - 1901):						
O₃	-0.80	-0.47	0.00	-0.11	-11.44	-11.65
CO₂	2.58	1.71	-0.01	8.07	9.25	17.22
CO₂ + O₃	1.79	1.19	-0.01	7.48	0.45	7.83
Relative diff. (%)	(%)	(%)	(%)	(%)	(%)	(%)
O₃	-8.84	-10.54	-8.55	-0.27	-9.09	-6.98
CO₂	28.51	38.34	-19.11	19.64	7.35	10.31
CO₂ + O₃	19.78	26.68	-23.48	18.20	0.36	4.69
Lower Sensitivity						
	GPP (Pg C yr ⁻¹)	NPP (Pg C yr ⁻¹)	g_s (m/s)	Veg C (Pg C)	Soil C (Pg C)	Land C (Pg C)
Value in 1901:	9.34	4.65	0.03319	41.1	126.4	167.5
Absolute diff. (2050 - 1901):						
O₃	-0.40	-0.27	0.00	-0.34	-4.32	-4.66
CO₂	2.50	1.66	-0.01	7.98	11.59	19.57
CO₂ + O₃	2.15	1.43	-0.01	7.32	7.54	14.85
Relative diff. (%)	(%)	(%)	(%)	(%)	(%)	(%)
O₃	-4.28	-5.81	-4.01	-0.83	-3.42	-2.78
CO₂	26.77	35.70	-20.10	19.42	9.17	11.68
CO₂ + O₃	23.02	30.75	-21.93	17.81	5.97	8.87

1670

1671 **Table S5.** Simulated changes in the European land carbon cycle due to changing O₃ and CO₂ concentrations.
 1672 Shown are changes in total carbon stocks (Land C), split into vegetation (Veg C) and soil (Soil C) carbon, and
 1673 gross primary productivity (GPP), net primary productivity (NPP) and conductance (g_s), between 1901 and 2050.

1674

1675

1676

1677

1678

1679
1680
1681
1682

	GPP_hi (Pg C yr ⁻¹)	GPP_low (Pg C yr ⁻¹)	LandC_hi (Pg C)	LandC_low (Pg C)
Value in 1901:	9.05	9.34	167.00	167.50
Value in 2050:				
CO₂	11.63	11.84	184.22	187.07
O₃	8.25	8.94	155.35	162.84
CO₂ + O₃	10.84	11.49	174.83	182.35
† % change due to O ₃ at PI CO ₂	-8.84	-4.28	-6.98	-2.78
‡ % change due to O ₃ at high CO ₂	-6.79	-2.96	-5.10	-2.52
†† Alleviation of O ₃ damage by CO ₂ increase (%)	2.05	1.33	1.88	0.26

1683

1684 **Table S6.** Percentage reduction in simulated GPP and Land C by 2050 due to future O₃ effects at pre-industrial
1685 (PI) CO₂ concentration, and under increasing future CO₂ concentration. The difference between these defines the
1686 alleviation of the O₃ effect by CO₂. **O₃** = Fixed 1901 CO₂, Varying O₃ ; **CO₂** = Varying CO₂, Fixed 1901 O₃ ;
1687 **CO₂ + O₃** = Varying CO₂, Varying O₃. Calculated as: †) O₃ effect with fixed pre-industrial CO₂:
1688 $100 * (\text{fixCO}_2_varO_3[2050] - \text{value}[1901]) / \text{value}[1901]$, where value[1901] represents the hypothetical value at
1689 2050 from a run with fixCO₂_fixO₃ which is equivalent to the initial state, i.e. the value in 1901 ; ‡) O₃ effect
1690 with increasing CO₂: $100 * (\text{varCO}_2_varO_3[2050] - \text{varCO}_2_fixO_3[2050]) / \text{varCO}_2_fixO_3[2050]$; ††) the alleviation
1691 of O₃ damage by CO₂ is the difference between the two runs: ‡ - †.

Commented [ORJ47]: RC1 14)

1692
1693
1694

1695

1696

1697

1698

1699 **Acknowledgments**

1700 This work used eddy covariance data acquired and shared by the FLUXNET community, including these
1701 networks: AmeriFlux, AfriFlux, AsiaFlux, CarboAfrica, CarboEuropeIP, CarboItaly, CarboMont, ChinaFlux,
1702 Fluxnet-Canada, GreenGrass, ICOS, KoFlux, LBA, NECC, OzFlux-TERN, TCOS-Siberia, and USCCC. The
1703 ERA-Interim reanalysis data are provided by ECMWF and processed by LSCE. The FLUXNET eddy covariance
1704 data processing and harmonization was carried out by the European Fluxes Database Cluster, AmeriFlux
1705 Management Project, and Fluxdata project of FLUXNET, with the support of CDIAC and ICOS Ecosystem
1706 Thematic Center, and the OzFlux, ChinaFlux and AsiaFlux offices.

1707 **References**

1708 B ker, P., Feng, Z., Uddling, J., Briolat, A., Alonso, R., Braun, S., Elvira, S., Gerosa, G., Karlsson, P. E.,
1709 Le Thiec, D., Marzuoli, R., Mills, G., Oksanen, E., Wieser, G., Wilkinson, M., and Emberson, L. D.: New
1710 flux based dose-response relationships for ozone for European forest tree species, *Environmental*
1711 *Pollution*, 163-174, 2015.
1712 CLRTAP: The UNECE Convention on Long-range Transboundary Air Pollution. Manual on
1713 Methodologies and Criteria for Modelling and Mapping Critical Loads and Levels and Air Pollution
1714 Effects, Risks and Trends: Chapter III Mapping Critical Levels for Vegetation, accessed via,
1715 [http://icpvegetation.ceh.ac.uk/publications/documents/Chapter3-](http://icpvegetation.ceh.ac.uk/publications/documents/Chapter3-Mappingcriticallevelsforvegetation_000.pdf)
1716 [Mappingcriticallevelsforvegetation_000.pdf](http://icpvegetation.ceh.ac.uk/publications/documents/Chapter3-Mappingcriticallevelsforvegetation_000.pdf), 2017.
1717 IGBP-DIS: International Geosphere-Biosphere Programme, Data and Information System, Potsdam,
1718 Germany. Available from Oak Ridge National Laboratory Distributed Active Archive Center, Oak
1719 Ridge, TN, available at: <http://www.daac.ornl.gov>,
1720 Jung, M., Reichstein, M., Margolis, H. A., Cescatti, A., Richardson, A. D., Arain, M. A., Arneth, A.,
1721 Bernhofer, C., Bonal, D., Chen, J., Gianelle, D., Gobron, N., Kiely, G., Kutsch, W., Lasslop, G., Law, B.
1722 E., Lindroth, A., Merbold, L., Montagnani, L., Moors, E. J., Papale, D., Sottocornola, M., Vaccari, F.,
1723 and Williams, C.: Global patterns of land-atmosphere fluxes of carbon dioxide, latent heat, and
1724 sensible heat derived from eddy covariance, satellite, and meteorological observations, *Journal of*
1725 *Geophysical Research: Biogeosciences*, 116, n/a-n/a, 10.1029/2010JG001566, 2011.
1726 Karlsson, P. E., Braun, S., Broadmeadow, M., Elvira, S., Emberson, L., Gimeno, B. S., Le Thiec, D.,
1727 Novak, K., Oksanen, E., Schaub, M., Uddling, J., and Wilkinson, M.: Risk assessments for forest trees:
1728 The performance of the ozone flux versus the AOT concepts, *Environmental Pollution*, 146, 608-616,
1729 <http://dx.doi.org/10.1016/j.envpol.2006.06.012>, 2007.
1730 O'Connor, F. M., Johnson, C. E., Morgenstern, O., Abraham, N. L., Braesicke, P., Dalvi, M., Folberth,
1731 G. A., Sanderson, M. G., Telford, P. J., Voulgarakis, A., Young, P. J., Zeng, G., Collins, W. J., and Pyle, J.
1732 A.: Evaluation of the new UKCA climate-composition model – Part 2: The Troposphere, *Geosci.*
1733 *Model Dev.*, 7, 41-91, 10.5194/gmd-7-41-2014, 2014.
1734 Tans, P., and Keeling, R.: Dr. Pieter Tans, NOAA/ESRL (www.esrl.noaa.gov/gmd/ccgg/trends/) and Dr.
1735 Ralph Keeling, Scripps Institution of Oceanography (scrippsco2.ucsd.edu/).
1736 Weedon, G. P.: Readme file for the "WFDEI" dataset.available at: [http://www.eu-](http://www.eu-watch.org/gfx_content/documents/README-WFDEI.pdf)
1737 [watch.org/gfx_content/documents/README-WFDEI.pdf](http://www.eu-watch.org/gfx_content/documents/README-WFDEI.pdf), 2013.

1738

1739